NEOPLASIA
www.neoplasia.com

Volume 16 Number 3 March 2014 pp. 265–278.e13 265

CTHRC1 Acts as a Prognostic Factor and Promotes Invasiveness of Gastrointestinal Stromal Tumors by Activating Wnt/PCP-Rho Signaling[1]

Ming-Ze Ma*,[2], Chun Zhuang†,[2], Xiao-Mei Yang*, Zi-Zhen Zhang†, Hong Ma*, Wen-Ming Zhang‡, Haiyan You*, Wenxin Qin*, Jianren Gu*, Shengli Yang*, Hui Cao† and Zhi-Gang Zhang*

*State Key Laboratory of Oncogenes and Related Genes, Shanghai Cancer Institute, Renji Hospital, Shanghai Jiao Tong University School of Medicine, Shanghai, China; †Department of General Surgery, Renji Hospital, Shanghai Jiao Tong University School of Medicine, Shanghai, China; ‡Department of Endoscopy, Cancer hospital, and Department of Oncology, Shanghai Medical College, Fudan University, Shanghai 200032, China

Abstract

Gastrointestinal stromal tumors (GISTs) are the major gastrointestinal mesenchymal tumors with a variable malignancy ranging from a curable disorder to highly malignant sarcomas. Metastasis and recurrence are the main causes of death in GIST patients. To further explore the mechanism of metastasis and to more accurately estimate the recurrence risk of GISTs after surgery, the clinical significance and functional role of collagen triple helix repeat containing-1 (CTHRC1) in GIST were investigated. We found that CTHRC1 expression was gradually elevated as the risk grade of NIH classification increased, and was closely correlated with disease-free survival and overall survival in 412 GIST patients. *In vitro* experiments showed that recombinant CTHRC1 protein promoted the migration and invasion capacities of primary GIST cells. A luciferase reporter assay and pull down assay demonstrated that recombinant CTHRC1 protein activated noncanonical Wnt/PCP-Rho signaling but inhibited canonical Wnt signaling. The pro-motility effect of CTHRC1 on GIST cells was reversed by using a Wnt5a neutralizing antibody and inhibitors of Rac1 or ROCK. Taken together, these data indicate that CTHRC1 may serve as a new predictor of recurrence risk and prognosis in post-operative GIST patients and may play an important role in facilitating GIST progression. Furthermore, CTHRC1 promotes GIST cell migration and invasion by activating Wnt/PCP-Rho signaling, suggesting that the CTHRC1-Wnt/PCP-Rho axis may be a new therapeutic target for interventions against GIST invasion and metastasis.

Neoplasia (2014) 16, 265–278.e13

Introduction

Gastrointestinal stromal tumors (GISTs) are mesenchymal neoplasms that usually arise in the stomach or small intestine and typically cause bleeding, anaemia and pain [1]. It is believed that GISTs originate from interstitial cells of Cajal [2] and may also derive from gastrointestinal smooth muscles or gut stem cells [3]. The pathological features of GISTs range from benign neoplasms to fatal sarcomas [1,4]. Most gastrointestinal stromal tumors stain positively for KIT [5,6], Ki67 [7] and anoctamin 1; exon mutations [6] in KIT or PDGFRA genes in approximately 80% or 10% of GISTs, respectively, have been demonstrated [1]. More than 60% of GIST patients can be cured by surgical resection [8,9]. The use of imatinib mesylate (Gleevec; Novartis) adjuvant treatment [8] is recommended in advanced GIST

Abbreviations: CTHRC1, collagen triple helix repeat containing 1; DFS, disease-free survival; ECM, extracellular matrix; GIST, gastrointestinal stromal tumors; OS, overall survival; qRT-PCR, quantitative real-time polymerase chain reaction

Address all correspondence to: Hui Cao, Department of General Surgery, Renji Hospital, Shanghai Jiao Tong University School of Medicine, 1630 Dongfang Road, Shanghai 200127, China or Zhi-Gang Zhang, State Key Laboratory of Oncogenes and Related Genes, Shanghai Cancer Institute, Renji Hospital, Shanghai Jiao Tong University School of Medicine, 800 Dongchuan Road, Shanghai 200240, China. E-mail: caohuishcn@hotmail.com; zzhang@shsci.org

[1] This article refers to supplementary materials, which is designated by Table W1 and Figures W1 to W3 is available online at www.neoplasia.com.

[2] These authors contributed equally to this work.

Received 10 February 2014; Revised 26 February 2014; Accepted 3 March 2014

http://dx.doi.org/10.1016/j.neo.2014.03.001

patients with postoperative recurrence risk, and the survival rate can be improved; however, secondary imatinib resistance is common [10].

Micrometastases and overt metastases are the main causes of death in malignant tumors, and this is the case in GIST patients as well [11,12]. Approximately 40% GISTs patients had metastatic lesions when definitively diagnosed, and more than 10% patients exhibited overt metastases [1]. Therefore, developing new predictors that can be used to estimate the risk of metastasis and postoperative recurrence is urgent.

Extracellular matrix (ECM) proteins play important roles in regulating tumor invasion and metastasis [13-15]. Given the secretary property, ECM proteins are also ideal candidates for tumor serum biomarkers and therapeutic targets.

Collagen triple helix repeat containing-1(CTHRC1) is a 28-kD extracellular matrix glycoprotein containing an NH2-terminal signaling peptide for extracellular secretion, a short collagen triple helix repeat of 36 amino acids, and a COOH-terminal globular domain [16].*CTHRC1* was initially found in a screen for differentially expressed genes in balloon-injured versus normal rat arteries [16]. It has been reported that the CTHRC1 protein positively regulates the Wnt-PCP pathway by stabilizing formation of the Wnt ligand and Frizzled receptor complex [17] in developmental morphogenesis [17]. CTHRC1 has recently been shown to be highly expressed in human pancreatic cancer tissues [18], hepatocellular carcinoma [13], gastric cancer [19], and colorectal cancer [20], and it promotes invasion and metastasis in these cancers. Several studies revealed that CTHRC1 regulates cancer cell motility and invasiveness through activating the Wnt-PCP pathway [18]. However, the clinical significance and functional role of CTHRC1 in GIST remain unclear. In this study, we first examined the expression of CTHRC1 and its correlation with the clinicopathological parameters of GIST. Then, we further analyzed the relationship between CTHRC1 expression and the survival of GISTs patients and identified CTHRC1 as a novel prognostic factor of GIST. Finally, we demonstrated that CTHRC1 promoted migration and invasion of primary GIST cells through activated Wnt/PCP-Rho signaling.

Materials and Methods

Ethics Statement

We obtained approval from the Regional Ethical Committees, Renji Hospital, School of Medicine, Shanghai Jiao Tong University, Shanghai, China for the use of clinical GIST patients' tissues. All the patients joined this study have signed informed consent. Ethical approval number, 2012031.

Patients

The inclusion criteria for our study were as follows: 1) a distinct pathologic diagnosis of GIST (CD117 positive in immunohistochemistry staining) ; 2) primary GIST cases without history of other solid tumors; 3) accepted radical surgery treatment without tumor residual; 4) without any chemotherapy, radiotherapy or other anticancer therapies before surgery; 5) availability of complete clinicopathologic and follow-up data; 6) obtained informed consent of patients and approval of the ethics committee of Renji Hospital for the use of samples. A total of 412 GIST cases, pathologic diagnosed and treated range from September 2004 to September 2013, were retrospectively identified from the hospitalization archives of Department of General Surgery, Renji Hospital, Shanghai, China. The paraffin-embedded tissue samples of these patients were used for tissue microarray construction and immunohistochemical staining. The clinicopathologic parameters include patients' age, gender, pathogenic site, histological type, tumor size (cm), number of mitoses/50 high-power fields (HPF), tumor rupture, mutation type and imatinib adjuvant treatment regimens. The risk of GIST behavior was classified into very low, low, intermediate, and high-risk categories according to the modified National Institute of Health (NIH) consensus [21,22]. In our study, the criterion of imatinib adjuvant therapy is at least twelve months uninterrupted drugs at a dose of 400mg/day. All the patients involved in our research accepted physical examination once a month during the first year after surgery and every six months thereafter. High risk GIST patients were accepted computed tomography (CT) or magnetic resonance imaging (MRI) of abdomen and pelvis at three-months intervals during the first three years after surgery, and subsequently at six-months intervals until five years after surgery. Complete follow-up data for GIST patients in cohort were available. Patients were followed until September 2013. Overall survival (OS) was defined as the time from surgery to death or the last follow-up examination. Disease free survival (DFS) was defined from the date of surgery until the detection of tumor recurrence or last observation.

Tissue Microarray Construction

Tissue microarrays were constructed by Suzhou Xinxin Biotechnology (Xinxin Biotechnology Co, Suzhou, China). Tissue paraffin blocks of GIST samples were stained with hematoxylin-eosin to confirm the diagnoses and marked at fixed points with most typical histological characteristics under a microscope. Two 1.6 mm cores per donor block were transferred into a recipient block tissue microarrayer, and each dot array contained fewer than one hundred and sixty dots. Three-micron-thick sections were cut from the recipient block and transferred onto glass slides using an adhesive tape transfer system for ultraviolet cross linkage.

Immunohistochemistry Stain

The tissue microarray glass slides were baked at 55°C for one hour, and then de-paraffinized gradually through xylene, 50% xylene, gradient concentrations of ethanol until immersed in tap water. Tissue sections were blocked for peroxidase activity with 0.3% Hydrogen peroxide at 37°C for 30mins. Antigen retrieval was carried out via boiling in 10mmol/L citrate buffer (pH6.0) for fifteen mins. Then the tissues were incubated with *CTHRC1* antibody (mouse monoclonal antibody, 1:100 dilution, Huaan Biotechnology, Hangzhou, China) overnight at 4°C. Next day, the tissues were washed with phosphate buffer solution (PBS) for three times and incubated with HRP-labelled anti-mouse secondary antibody (1:200dilution, Dako, Carpinteria , CA, USA) for one hour at room temperature. Immunostaining was carried out using diaminobenzidine substrate chromogen (Dako, Carpinteria, CA, USA) method and chromogenic reaction was controlled under microscope. After immunostaining, tissues were immersed into hematoxylin for nuclear staining. The TMA slides were then dehydrated through gradient concentrations of ethanol, cleared with xylene, and coverslipped with neutral balsam (Shenggong , Shanghai, China). The staining results were judged by two pathologists according to criterion as follows: 0: weak, no staining was observed; 1+, 25% to 50% of the tumor cells were weak or moderate staining; 2+, strong, more than 50% tumor cells were moderate or strong staining. 1+ and 2+ scores were identified as positive staining, while 0 score means negative staining. Negative controls for primary and secondary antibodies were shown in Figure W3. *Total RNA Extraction*

and Quantitative Real-time PCR Total RNA was extracted from 29 fresh GIST tissues using Trizol reagent (Takara, Dalian, China) followed the manufacturer instructions. The reverse-transcription reactions were carried out with random primers and M-MLV Reverse Transcriptase (Takara, Dalian, China). The 29 cases of cDNA were used for templates of quantitative real-time PCR reaction in SYBR-Green method. All the qPCR reactions were performed on a StepOne^{TM} real-time PCR System (Applied Biosystems, Foster City, CA,USA). *Beta-actin* was used as an internal control. The $2^{-\triangle Ct}$ method was used to quantify the relative *CTHRC1* expression levels. The forward and reverse *CTHRC1* primer sequences were: 5′-TGGTATTTCACATTCAATGGAGCTG-3′ and 5′-TGGGTA- -ATCTGAACAAGTGCCAAC-3′, respectively.

Western Blotting

Fresh GIST tissues were lysed in tissue protein extraction reagent (Invitrogen). Primary GIST cells were lysed in Western and IP lysis buffer (P0013, Beyotime, Jiangsu, China) supplemented with 1mM PMSF (Adamas beta, Shanghai, China). The lysis buffer includes, 20mM Tris (pH7.5), 150mM NaCl, 1%Triton X-100, sodium pyrophosphate, β-glycerophosphate, EDTA, Na3VO4, leupeptin. Proteins were separated by 10% SDS-PAGE under reducing condition, followed by blocking in phosphate-buffered saline/Tween-20 containing 1%BSA (Bovine Serum Albumin). The NC (Nitrocellulose filter membrane) or PVDF (Polyvinylidenefluoride) membrane was incubated with antibodies for CTHRC1(1:1000, mouse, Huaan, Hangzhou, China) , JNK (1:1000, Rabbit source, Cell Signaling Technology), RhoA (1:1000,Rabbit,CST), Rac1(1:1000,Mouse, Millipore) ,Cdc42 (1:1000,Mouse) and species-specific secondary antibodies. Bound the IRDye 680 anti-mouse (LI-COR, 1:20000) and IRDye 800 anti-rabbit (LI-COR, 1:10000) secondary antibodies were revealed by Odyssey imaging system (LI-COR). Wnt5a neutralizing antibody (R&D), Wnt3a neutralizing antibody (R&D), NSC23766 (Rac1 inhibitor, Merck Millipore, effective dose: 50 μM), Y-27632 (ROCK inhibitor, effective dose: 100 μM).

CTHRC1 Recombinant Protein Expression, Purification and Verification

CTHRC1 ORF were cloned into the episomal expression vector V152 (Figure W1B) with pCEP-Pu-Strep II-tag (C-terminal) in-frame and the sequence of the BM-40 (SPARC/osteonectin) signal

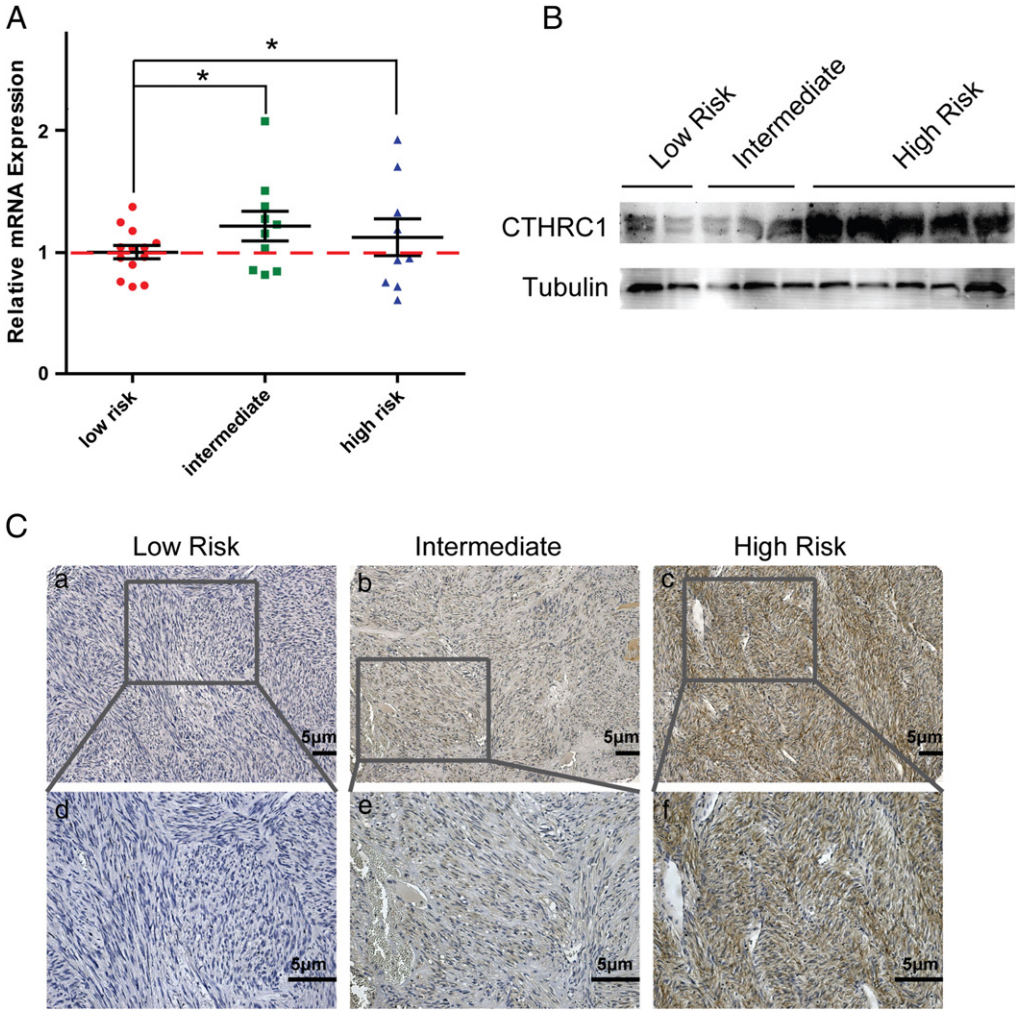

Figure 1. CTHRC1 expression in GIST tissues. (A) Relative mRNA expression of *CTHRC1* in low-risk group was significantly lower than those in the intermediate- and high-risk groups. (B) Western blotting analysis showed that CTHRC1 expression in high-risk GIST patients was significantly higher than those of low-risk or intermediate-risk groups. Tubulin was included as a loading control. (C) Representative image of immunohistochemical staining of CTHRC1 in low-risk, intermediate-risk and high-risk GIST tissues. Original magnification: a, b, c, 100×; d, e, f, 200×. Scale bars, 5 μm (*, $P < 0.05$).

peptide downstream of the CMV promoter. CTHRC1 was recombinant expressed in EBNA-293 cells after transfecting reconstructed plasmid by using X-tremeGENE 9 DNA Transfecting Reagent (Roche, Mannheim, Germany). Forty eight hours after transfection, the EBNA-293 cells were screening with puromycin (Sigma-Aldrich, St. Louis, MO) at a dose of 2μg/ml in DMEM supplemented with 10% FBS for seven days, then the culture media were collected and applied to the Strep Tactin sepharose column(IBA, Gottingen, Germany). After this, the column was washed with binding buffer and eluted by elution buffer containing 2.5 mM desthiobiotin. The collected fractions were further quantified by Nanodrop 2000 spectrophotometer (Thermo Fisher Scientific, Wilmington, DE) and BCA Protein Assay Kit (Pierce. Biotechnology Inc, Rockford, IL) and identified by western blotting assay.

In Vitro Migration and Invasion Assays

For the transwell migration assay, 4×10^4 primary GIST cells were placed on the top chamber of each insert with the noncoated membrane (Millicell). Cells were trypsinized and resuspended in DMEM and 700-900μL of medium supplemented with 10% fetal bovine serum added rCTHRC1 protein followed gradient doses of 0 nM, 1 nM, 20 nM, 50 nM respectively were injected into the lower chamber. After 24 hours for GIST cells in the migration assays, any cells remaining in the top chambers or on the upper membrane of the inserts were carefully removed. After fixation and staining in a dye solution containing 0.1% crystal violet and 20% methanol, cells adhering to the lower membrane of the inserts were counted and imaged through an IX71 inverted microscope (Olympus Corp. Tokyo, Japan). We carried out invasion assay by adding 100μl matrigel (BD Bioscience, Franklin Lakes, NJ) into top chamber of transwell and placed 8×10^4 primary GIST cells onto the matrigel. 48 hours later, the transwell for invasion was ceased and staining.

Cell Viability Assay

Cell viability was detected using a standard Cell Counting Kit-8 assay. Primary GIST cells were seeded into 96-well plates (100μl per well) at a density of 3×10^4 cells per ml. Cells in four divided groups were added rCTHRC1 protein followed gradient doses of 0 nM, 1 nM, 20 nM, 50 nM respectively. We added 10μl of reagent from Cell Counting Kit-8 (Dojindo, Kumamoto, Japan) to each well for detection at day 1, 2, 3, 4, 5. After two hours of incubation at 37°C, the optical density was measured using microplate reader at a wavelength of 450nm.

Cell Isolation and Primary Cell Culture

Fresh surgical GIST tissues were gently minced with scissors, washed twice with phosphate-buffered saline (PBS), and then filtered through the steel mesh with 200 μm pore diameter. After washed in cold PBS, cell pellets were resuspended in RPMI-1640 medium supplemented with 20% fetal calf serum (FCS; Gibco, France) and seeded onto culture dishes. The primary GIST cells were cultured in incubator with 5%CO2 and 37 degrees centigrade. The culture medium for primary GIST cells were changed twice every three days . The successfully isolated primary GIST cells were shown in Figure 3*A*.

Pull Down Assay

Pull down assays were conducted as reported [23] . Primary GSIT cells cultured in 100 mm dishes were serum-starved for 24 hours and treated with rCTHRC1 at a dose of 20 nM or desthiobiotin buffer for 2 hours. The primary antibodies used included the following: mouse primary antibody against Rac1 (Millipore, 1:1000) and rabbit primary antibody against RhoA, Cdc42 (Cell Signaling Technology, 1:1000).

Luciferase Reporter Assay

Primary GIST cells were seeded in 96-well plates and transfected with mixture of 100 ng TCF/catenin reporter plasmid (Wnt/β-catenin signaling), or 100 ng ATF2 reporter plasmid (Wnt/PCP signaling), and 10 ng Renilla following the recommended protocol for the Lipofectamine 2000 transfection system. One group of GIST cells were treated with rCTHRC1 protein at a concentration of 20 nM. After 48 hours of incubation, firefly and Renilla luciferase activities were measured using the dual-luciferase reporter assay system (Promega, Madison, WI) from the cell lysates.

Statistical Analysis

Statistical analyses were conducted using SPSS 16.0 software (Chicago, IL, USA). We performed chi-squared tests in cross tables to assess the relationships between expression levels of *CTHRC1* and clinicopathological factors. Overall survival (OS) and Disease-free survival (DFS) were calculated using Kaplan-Meier method. The survival distributions were compared through log-rank test. All statistical tests were two-sided. One-way analysis of variance (ANOVA, Post-hoc testing) was used to compare groups (Table W1). *P* value less than 0.05 was considered statistically significant.

Results

CTHRC1 Expression Is Gradually Elevated in Accordance with GIST Risk Grades

To investigate the *CTHRC1* expression level in GIST tumor tissues with different risk grades, we first evaluated the mRNA

Table 1. Relationship between CTHRC1 expression and clinicopathologic features of GIST patients(*, $P < 0.05$; **, $P < 0.01$).

Variable		CTHRC1(n = 412)		
		Low	High	*P*
Age [$]	≤59 years	31	49	0.458
	>59 years	114	218	
Gender	Male	65	158	0.005
	Female	80	109	
Tumor site	Stomach	100	128	**<0.001**
	Small bowel	28	93	
	Colon	12	9	
	Other sites	5	37	
Tumor size(cm)	≤2	30	7	**<0.001**
	>2&≤5	102	61	
	>5&≤10	9	127	
	>10	4	72	
Mitoses per 50 HPFs	≤5	138	170	**<0.001**
	>5&≤10	2	52	
	>10	5	45	
Modified NIH criteria	Very low risk	30	2	**<0.001**
	Low risk	101	51	
	Intermediate risk	4	58	
	High risk	10	156	
NIH invasion	1	30	2	**<0.001**
	2	101	51	
	3	4	58	
	4	5	101	
	5	5	55	
Tumor bleeding	No	131	220	0.030
	Yes	14	47	

Abbreviations: HPF, high power field of the microscope; NIH, National Institutes of Health.
The P value in bold emphasize statistical significance (P<0.001).
[$] Median age of total 412 patients was 59 years.

expression level of *CTHRC1* in fresh GIST tissue samples by quantitative PCR (qPCR). The results showed that *CTHRC1* mRNA expression levels in GIST tumor tissues of the intermediate- and high-risk groups were higher than those of the low-risk group (Figure 1*A*). We further compared the protein expression level of CTHRC1 in GIST tissues with different risk grades. The three low-risk, two intermediate-risk and five high-risk samples were analyzed by western blotting. The results showed that the CTHRC1 protein expression level in the high-risk group was significantly higher than that of the intermediate- and low-risk groups (Figure 1*B*).

CTHRC1 Protein Expression Level Is Closely Correlated with Risk Grade of NIH Classification, and Prognosis of GIST

The clinicopathological significance of CTHRC1 was further examined using a tissue microarray which contained 412 GIST tissue samples. The immunohistochemistry staining results showed that 145 (35.2%) cases showed CTHRC1 low expression, 267 (64.8%) cases showed CTHRC1 high expression (Figure 1*C*). The correlations between CTHRC1 expression and the clinicopathological parameters are shown in Table 1. We found that the expression level of CTHRC1 was higher in the patients with high NIH grade, large tumor size (>10 cm) or increased mitotic figures than those with low NIH grade, small tumor size (<10 cm), fewer mitotic figures with statistical significance ($P < 0.05$). Interestingly, we found that there was a significant difference between male (70.85%) and female (57.67%) GIST patients in frequency of high CTHRC1 levels. The statistical analysis suggested that CTHRC1 expression was not correlated with age, histological type, or tumor rupture. We further investigated the correlation between CTHRC1 expression and overall survival (OS) or disease-free survival (DFS) of GIST patients. The OS in the CTHRC1 negative (low) group (five-year OS rates, 100%, 145/145) was remarkably superior than that in the CTHRC1 positive (high) expression group (five-year OS rates, 90.6%, 242/267) (Figure 2*A*). The DFS in the CTHRC1 negative (low) group (five-year DFS rates, 95.2%, 138/145) was significantly higher than that in the CTHRC1 positive (high) expression group (five-year DFS rates, 76.8%, 205/267) (Figure 2*B*). In summary, CTHRC1 expression in GIST tumor tissues was closely correlated with OS and DFS of GIST patients.

Correlation between CTHRC1 Expression and the Efficacy of Imatinib Adjuvant Treatment

According to the NIH classification guideline, intermediate- or high-risk GIST patients require adjuvant treatment with imatinib. In

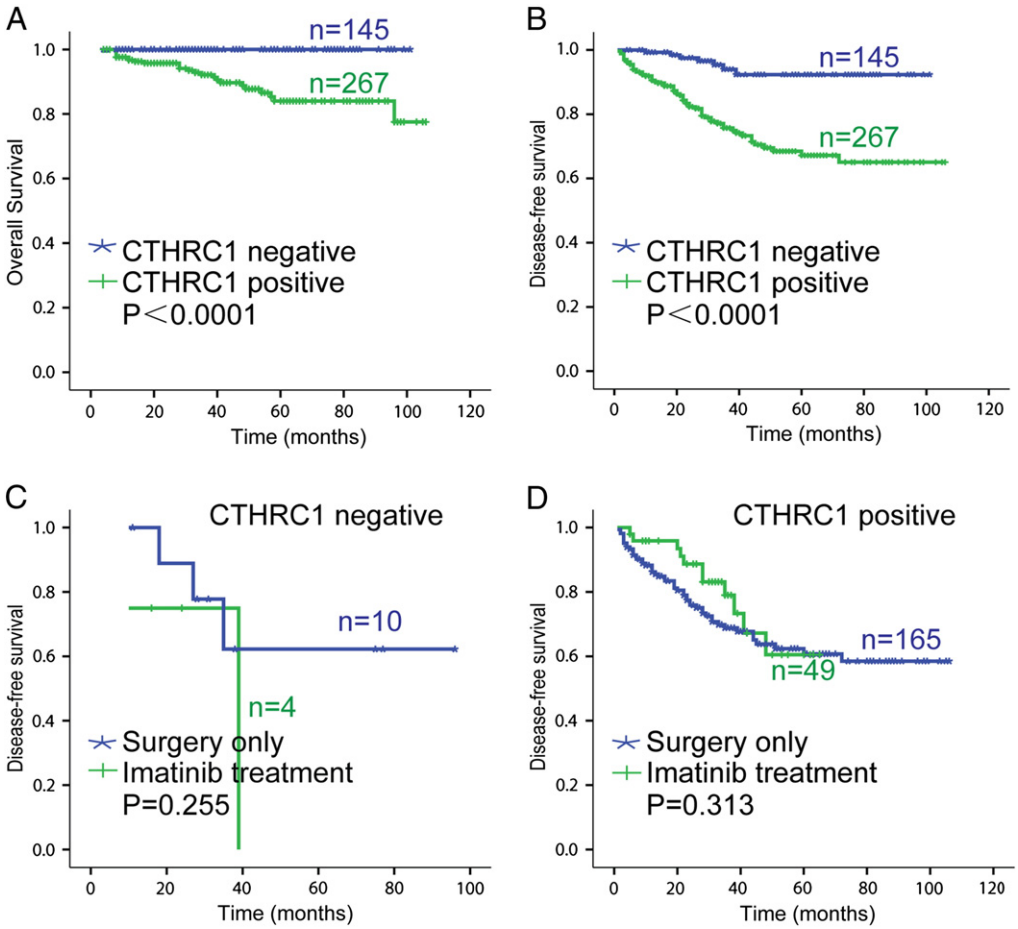

Figure 2. (A) Kaplan-Meier analysis of overall survival related to the expression of CTHRC1 in 412 GIST patients. (B) Kaplan-Meier analysis of disease-free survival related to the expression of CTHRC1 in 412 GIST patients. (C) Among CTHRC1-negative intermediate- and high-risk GIST patients, there was no significant difference in DFS between the groups with or without imatinib adjuvant treatment. (D) Among CTHRC1-positive intermediate- and high-risk GIST patients, no significant difference between the imatinib treatment group and the surgery alone group were observed.

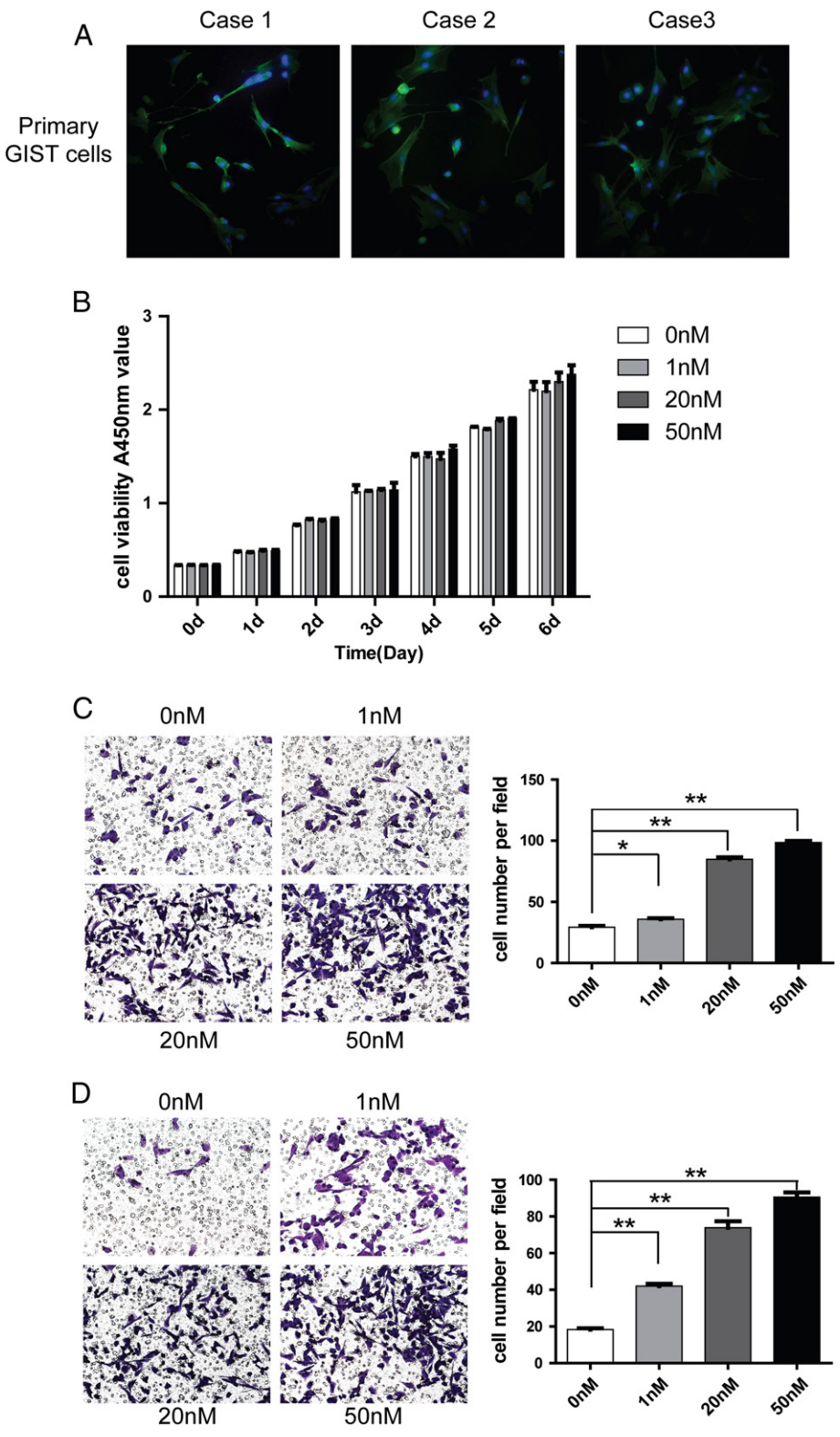

Figure 3. (A) Immunofluorescent staining showed the morphology of primary GIST cells isolated from the GIST tissues of three patients. The green fluorescence represents phalloidin for F-actin staining, whereas the blue fluorescence represents DAPI for nuclear staining. (B) Cell viability of primary GIST cells treated with rCTHRC1 protein at doses of 0 nM, 1 nM, 20 nM, 50 nM were measured using CCK-8 assay for six days. (C) Representative images (left) of GIST cells that migrated to the bottom of transwell filter (8μm, pore diameter) and statistical analysis (right) of the cell migration stimulated with rCTHRC1 protein or vehicle. (D) Representative images (left) of GIST cells that invaded through Matrigel to the bottom of transwell filter (8μm, pore diameter) and statistical analysis (right) of the cell invasiveness stimulated with rCTHRC1 protein or vehicle. The results shown are mean±SD of migration, and invading cells were photographed at 200× magnification per field. (*, $P < 0.05$; **, $P < 0.01$).

this study, we analyzed the correlation between the efficacy of imatinib adjuvant treatment and CTHRC1 expression. Among 14 CTHRC1- negative intermediate- and high-risk GIST patients, there was no correlation between imatinib treatment and patient prognosis (Figure 2*C*). The difference in DFS between the imatinib treatment group and the surgery treatment only group was not statistically significant (P = 0.255). Notably, among 214 CTHRC1- positive intermediate- and high-risk GIST patients, the DFS rate in the imatinib treatment group were higher than that in the surgery only group within 3 years of follow-up. However, the differences in 5-year DFS rates in the two groups were not statistically significant (P = 0.313) (Figure 2*D*). Therefore, the expression of CTHRC1 can not predict the efficacy of imatinib adjuvant treatment in our current study.

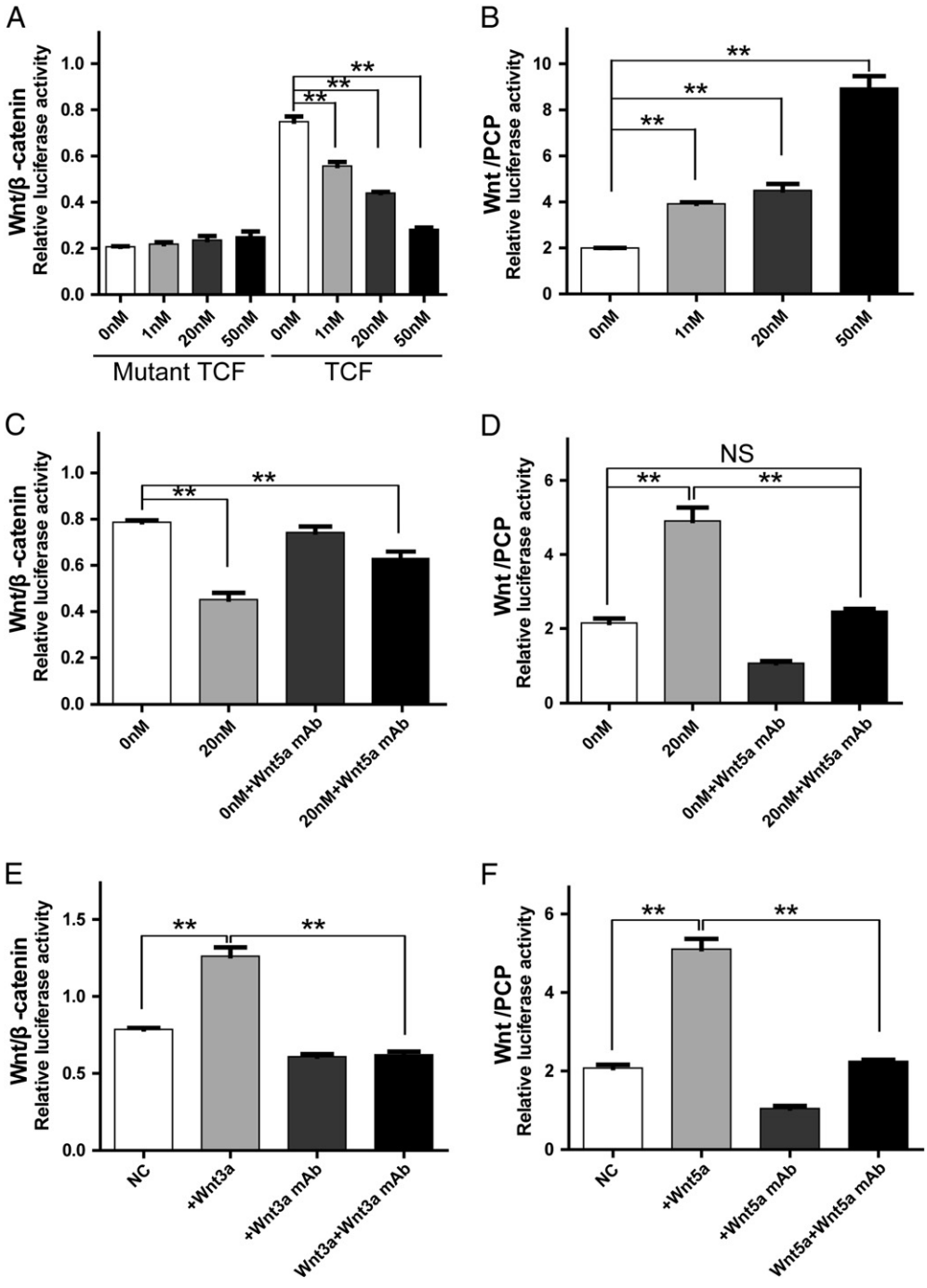

Figure 4. (A) Dual-luciferase reporter assay showed that rCthrc protein inhibited Wnt/β-catenin signaling of primary GIST cells in a dose-dependent manner. The results shown are mean ± SD of relative firefly/Renilla ratio. (B) Noncanonical Wnt/PCP signaling of GIST cells was activated by rCTHRC1 protein in a dose-dependent manner. (C) The inhibitory effect of rCTHRC1 on Wnt/β-catenin signaling was partially blocked by Wnt5a monoclonal neutralizing antibody. (D) The promoting effect of rCTHRC1 protein on Wnt/PCP signaling was almost blocked by Wnt5a monoclonal neutralizing antibody. (E) The promoting effect of Wnt3a on Wnt/β-catenin signaling was almost blocked by Wnt3a monoclonal neutralizing antibody. (F) The promoting effect of Wnt5a on Wnt/PCP signaling was almost blocked by Wnt5a monoclonal neutralizing antibody. (*, $P < 0.05$; **, $P < 0.01$).

Recombinant CTHRC1 Protein Promotes GIST Cell Migration and Invasion in a Dose-dependent Manner

To explore the biological functions of CTHRC1 as a secreted protein, CTHRC1 was recombinantly expressed in EBNA-293 cells, and further purified and verified by western blotting (Figure W2). Then, the purified recombinant CTHRC1 (rCTHRC1) protein was applied to primary GIST cells in a migration and Matrigel invasion assay. Compared to the vehicle group, GIST cell migration and invasion were significantly enhanced by rCTHRC1 protein at doses of 1 nM, 20 nM, and 50 nM (Figure 3, *C* and *D*). Moreover, the promotion of cell motility by the rCTHRC1 protein was dose-dependent. However, primary cell viability was not remarkably affected by rCTHRC1 protein based on the cell viability assay (Figure 3*B*). These results demonstrate that CTHRC1 is a potent pro-invasion factor that facilitates GIST cell invasion in a dose-dependent manner.

CTHRC1 Activates Wnt/PCP-Rho Signaling in Primary GIST Cells

To understand the underlying mechanism by which CTHRC1 promotes GIST cell migration and invasion, we examined the activation of the canonical Wnt pathway and the non-canonical Wnt pathway. GIST cells were transfected with a Wnt//β-catenin reporter plasmid (TCF/catenin plasmid) and negative control counterpart plasmid or non-canonical Wnt/PCP pathway reporter plasmid (ATF2 plasmid). Recombinant CTHRC1 or vehicle control was added 24 hours after transfection, and luciferase activity was determined. The results showed that Wnt/β-catenin signaling was inhibited while the noncanonical Wnt/PCP signaling was activated by rCTHRC1 protein in primary GIST cells (Figure 4, *A* and *B*). The effects of rCTHRC1 protein on Wnt signaling was blocked by a Wnt5a neutralizing antibody (Figure 4, *C* and *D*). We also verified the block effect of Wnt3a and Wnt5a neutralizing antibodies (Figure 4, *E* and *F*). We further confirmed the

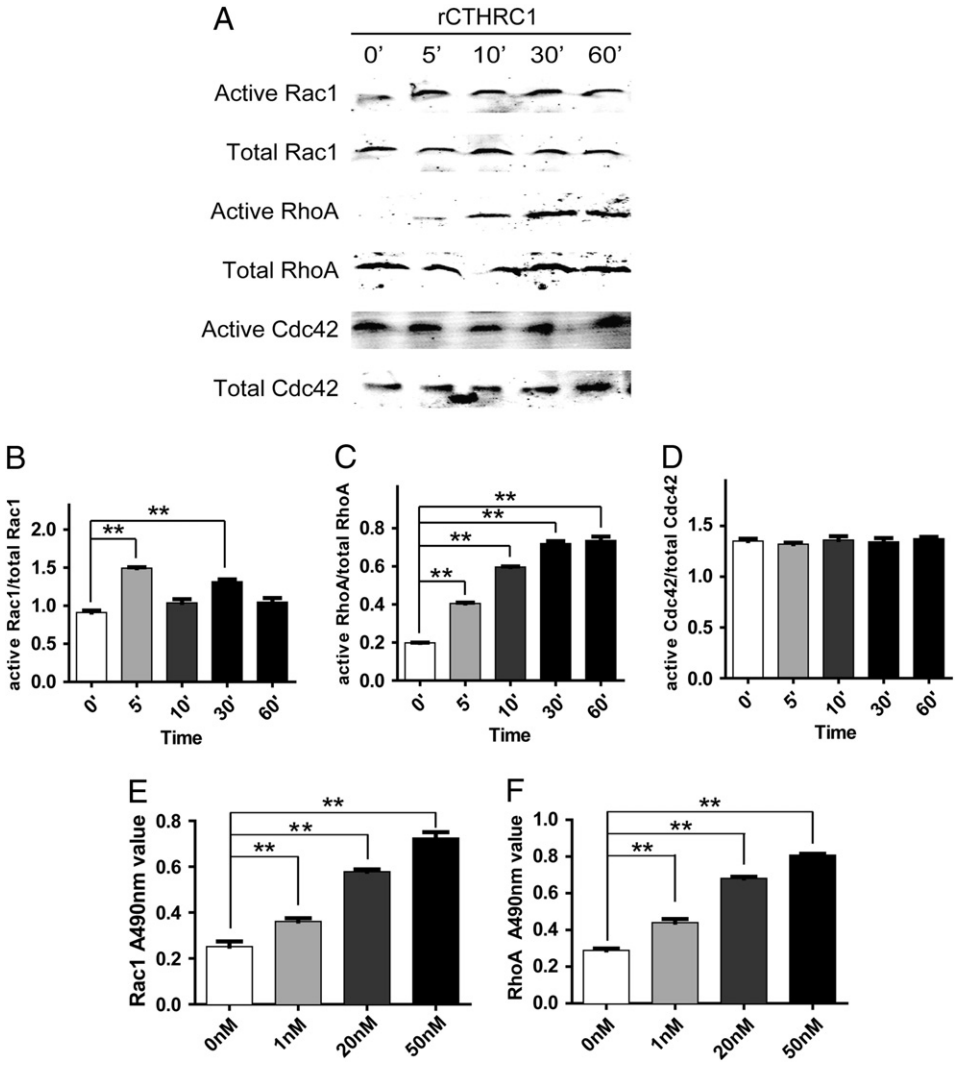

Figure 5. (A) Analysis of the active and total RhoA,Rac1 and Cdc42 in primary GIST cells treated with rCTHRC1 protein by pull-down assay.(B) Quantitative analysis of grey value for active Rac1/ -total Rac1 ratio using ImageJ software. (C) Quantitative analysis of grey value for active RhoA/ -total RhoA ratio using ImageJ software. (D) Quantitative analysis of grey value for active Cdc42/ total Cdc42 ratio using ImageJ software. (E) Rac1 G-LISA assay was used to assess the levels of GTP-bound Rac1 in GIST cells treated with rCTHRC1 protein. (F) RhoA G-LISA assay was used to assess the levels of GTP-bound RhoA in GIST cells treated with rCTHRC1 protein. (*, $P < 0.05$; **, $P < 0.01$).

inhibitory effect of CTHRC1 on Wnt/β-catenin signaling using western blotting assy. The level of phosphorylated β-catenin, which indicates the degradation of β-catenin, was increased in primary GIST cells treated with rCTHRC1 (Figure 6, *B* and *F*). In addition, the level of GSK3β, which phosphorylates β-catenin on Ser-33/Ser-37/Thr-41 was increased in rCTHRC1 treated primary GIST cells (Figure 6, *B* and *D*). Therefore, we confirmed that CTHRC1 inhibits the canonical Wnt/β-catenin pathway in primary GIST cells.

The downstream molecules of the Wnt/PCP pathway mainly include the small GTPase family, such as Rac1, RhoA and Cdc42, which play important roles in cancer cell migration and invasion. Using a Rho GTPases pull-down assay, we found that the rCTHRC1 protein enhanced the activity of RhoA and Rac1 but not Cdc42 (Figure 5, *A-D*).

To further confirm the above results, the GLISA assay, another approach to measure the activities of Rho GTPases, was performed. It also demonstrated that the activities of RhoA and Rac1 were significantly enhanced by rCTHRC1 treatment in primary GIST cells, which is consistent with the results of the Rho GTPases pull-down assay (Figure 5, *E* and *F*).

Furthermore, the phosphorylation of c-Jun N terminal kinase (JNK), another downstream molecule of the Wnt/PCP pathway, and Wnt5a were also elevated by rCTHRC1 treatment (Figure 6, *A*, *C* and *E*). These results suggested that CTHRC1 may promote GIST cell invasion through the Wnt/PCP-Rho-JNK pathway.

CTHRC1-induced Primary GIST Cell Migration and Invasion Is Wnt5a and Wnt/PCP Signaling-dependent

We further investigated whether Wnt3a (a ligand of canonical Wnt/β-catenin pathway) and Wnt5a (a ligand of noncanonical Wnt/PCP pathway) are involved in CTHRC1-induced GIST cell migration and invasion by using neutralizing antibodies of Wnt3a and Wnt5a. The data illustrated that the migration- and invasion-promoting activities of rCTHRC1 at a dose of 20 nM were not

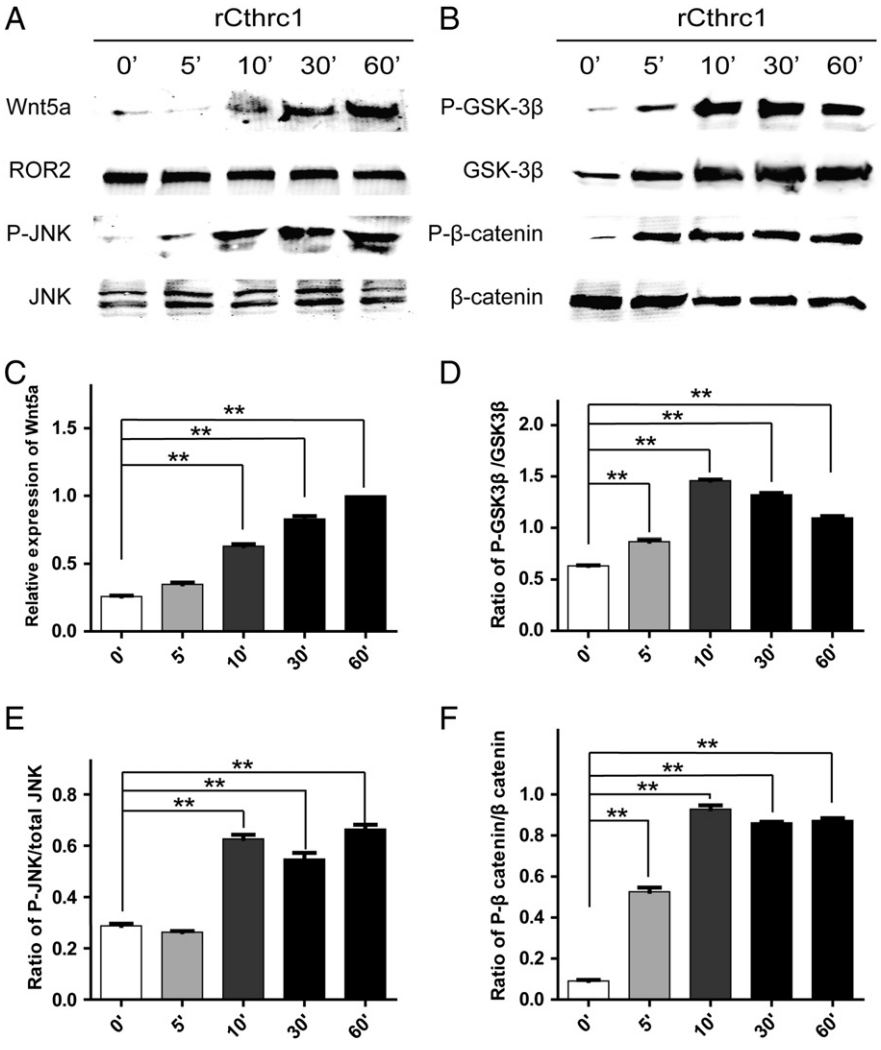

Figure 6. (A) The expression of Wnt5a and the phosphorylation of JNK were examined after treatment with rCTHRC1 by western blotting. (B) The phosphorylation of GSK3β and β-catenin were examined after treatment with rCTHRC1 by western blotting. (C) Quantitative analysis of grey value for Wnt5a using ImageJ software. The relative expression of Wnt5a induced by rCTHRC1 at 0′, 5′, 10′, 30′ was compared with the grey value of Wnt5a induced by rCTHRC1 at 60′. (D) Quantitative analysis of grey value for phospho-GSK3β/total GSK3β ratio using ImageJ software. (E) Quantitative analysis of grey value for phospho-JNK/total JNK ratio using ImageJ software. (F) Quantitative analysis of grey value for phospho-β-catenin/totalβ-catenin ratio using ImageJ software. (*, $P < 0.05$; **, $P < 0.01$).

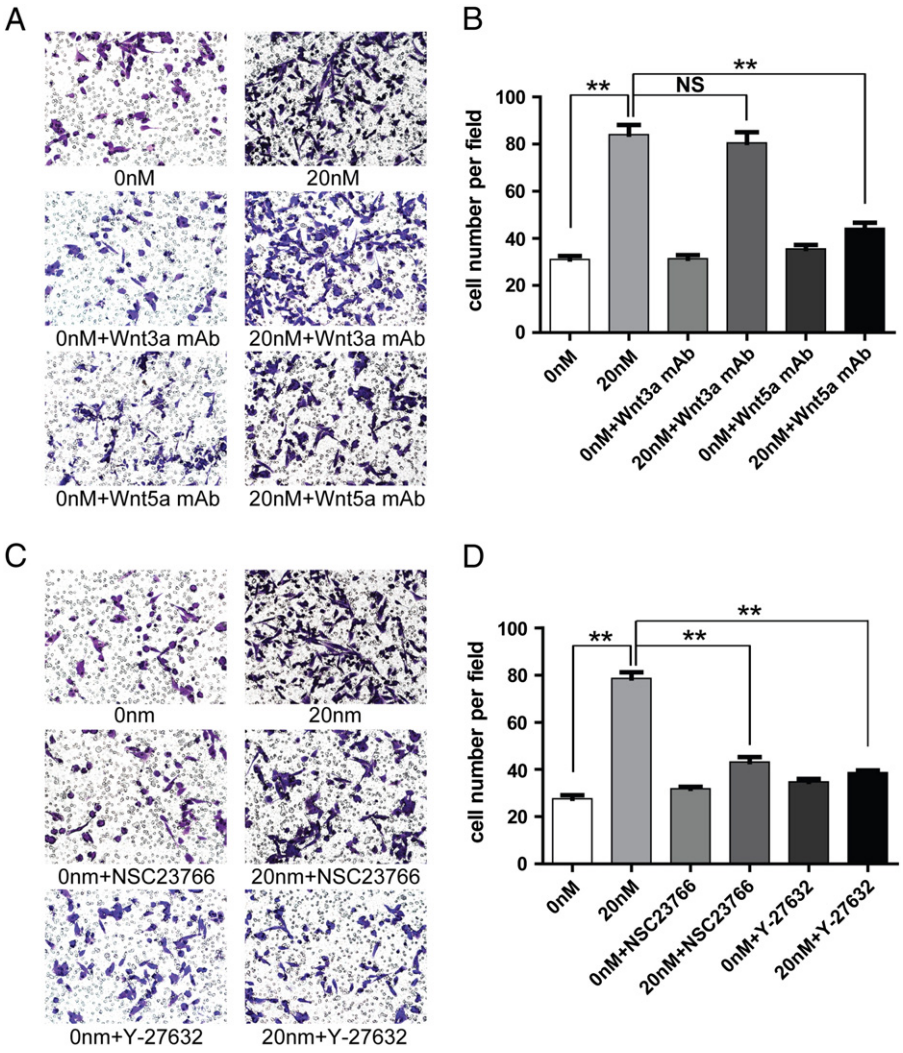

Figure 7. (A) The promotive effect of rCTHRC1 protein was blocked by Wnt5a neutralizing antibody but not blocked by Wnt3a neutralizing antibody shown from cell migration assay in vitro. (B) Quantification analysis of migrated cells were performed for six randomly selected fields (original magnification:200 ×). (C) The promotive effect of rCTHRC1 protein was partially blocked by Rac1 inhibitor (NSC23766) as well as ROCK inhibitor (Y-27632) shown from cell migration assay. (D) Quantification analysis of migrated cells were performed for six randomly selected fields (original magnification:200 ×). (*, $P < 0.05$; **, $P < 0.01$).

affected by the Wnt3a neutralizing antibody (Figure 7, *A* and *B*, Figure 8, *A* and *B*). However, the promoting effects of rCTHRC1 on GIST cell migration and invasion were almost completely blocked by the Wnt5a neutralizing antibody (Figure 7, *A* and *B*, Figure 8, *A* and *B*). We further investigated whether the promoting effects of CTHRC1 on GIST cells motility are Wnt/PCP signaling-dependent by using inhibitors of ROCK and Rac1, which are key downstream molecules of the Wnt/PCP pathway. The results showed that both ROCK and Rac1 inhibitors treatment inhibits the promoting effects of rCTHRC1 on GIST cell migration and invasion (Figure 7, *C* and *D*, Figure 8, *C* and *D*).

Taken together, these data indicated that the CTHRC1-induced GIST cell migration and invasion is Wnt5a and noncanonical Wnt/PCP signaling dependent (Figure 9).

Discussion

GISTs have a variable malignancy degree ranging from a curable disorder to highly malignant sarcomas [1,8]. The majority of GISTs stain positive for KIT oncoproteins in immunohistochemical assays [3,24]. KIT is a stem cell growth factor receptor that plays pro-proliferative and anti-apoptotic roles in GIST progression [5,6]. GIST patients treated with the KIT targeted inhibitor, – imatinib, showed prolonged median recurrence-free survival of 12 to 24 months [1,21]. Recurrence and metastasis in GIST patients are the major causes of treatment failure or even death [7,25,26]. Thus, new predictive biomarkers for recurrence and an understanding of the mechanisms of GIST metastasis are urgently needed.

By analyzing the GIST microarray dataset (GSE21315) from the GEO database (Figure W1*A*), we found that *CTHRC1* expression in GIST with liver metastasis was remarkably higher than in primary GIST tissues(fold change>3, $P < 0.05$). This result strongly suggested that CTHRC1 may play important roles in regulating GIST metastasis. The NIH classification published in 2002 was widely accepted as standard for predicting the prognosis of GIST patients [27,28]. According to the NIH classification, the risk assessments are based on tumor size and the number of mitotic figures. We have analyzed the correlation between CTHRC1 expression and GIST clinicopathological parameters and found that the CTHRC1

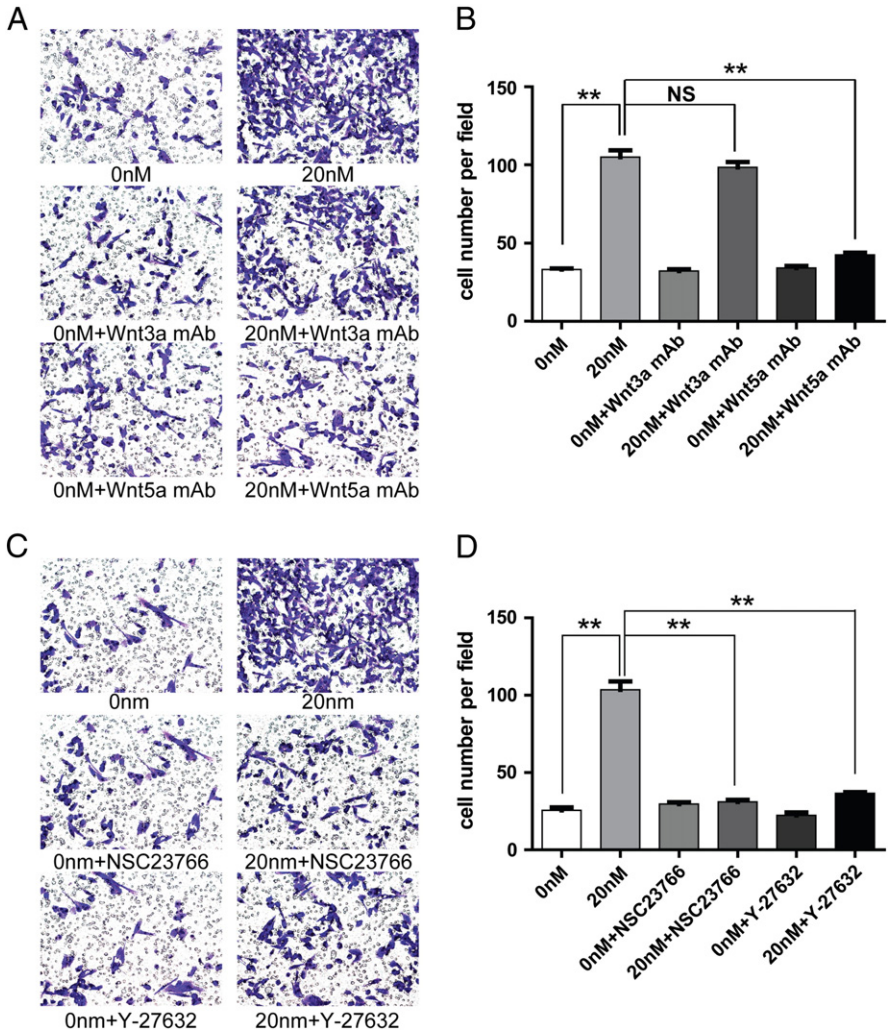

Figure 8. (A) The pro-invasion effect of rCTHRC1 protein was blocked by Wnt5a neutralizing antibody but not blocked by Wnt3a neutralizing antibody shown from cell invasion assay in vitro. (B) Quantification analysis of migrated cells were performed for six randomly selected fields (original magnification: 200×). (C) The pro-invasion effect of rCTHRC1 protein was partially blocked by Rac1 inhibitor (NSC23766) as well as ROCK inhibitor (Y-27632) shown from cell invasion assay. (D) Quantification analysis of migrated cells were performed for six randomly selected fields (original magnification:200×). (*, $P < 0.05$; **, $P < 0.01$).

expression levels were closely related to NIH classification, tumor size and the number of mitotic figures. These analyses suggest that CTHRC1-positive GISTs exhibit a greater likelihood of malignant behavior and more aggressive features. Moreover, there was a significant difference between male and female GIST patients in frequency of high CTHRC1 levels (Table 1). It has been reported that *CTHRC1* is associated with attenuated inflammatory arthritis severity in males, but not in females [29,30]. The naive mice assay showed that the expression and inducibility of *CTHRC1* were highly dependent on sex [29,30]. Among naive wild-type BALB/c mice, *CTHRC1* expression was remarkably higher in males than in females. Moreover, *CTHRC1* was one of the major sex-affected differentially expressed genes [29,30]. Therefore, sex disparities may cause the difference between male and female GIST patients in high CTHRC1 expression rates.

The Kaplan-Meier curves analysis revealed that CTHRC1 expression was closely correlated with OS and DFS of GIST patients. GIST patients with CTHRC1-positive tumors had shorter OS and DFS than CTHRC1-negative patients. Therefore, we identified that CTHRC1 is an available predictor of poor prognosis including OS and DFS in GIST patients. In addition, the great clinical value of CTHRC1 in predicting the recurrence risk of postoperative GIST patients may contribute to improving the clinical therapeutic effects.

Tumor microenvironments including components of extracellular matrix protein play crucial roles in promoting tumor invasion and metastasis [31]. CTHRC1, a secreted ECM protein, has been reported to be up-regulated in many solid tumors. In hepatocellular carcinoma, CTHRC1 is up-regulated and promotes tumor invasion and predicts poor prognosis [13]. CTHRC1 plays a promoting role in pancreatic cancer progression and metastasis by enhancing the migration ability of cancer cells [18]. These accumulating data indicate that CTHRC1 is an important regulator of tumor invasion and metastasis in the tumor microenvironment. In the present study, we have found that CTHRC1 expression in GIST tissue is gradually elevated in accordance with risk grading. Based on an *in vitro* functional assay, CTHRC1 was considered to be an invasion-promoting protein and ultimately contributed to gastrointestinal stromal tumor metastasis and recurrence.

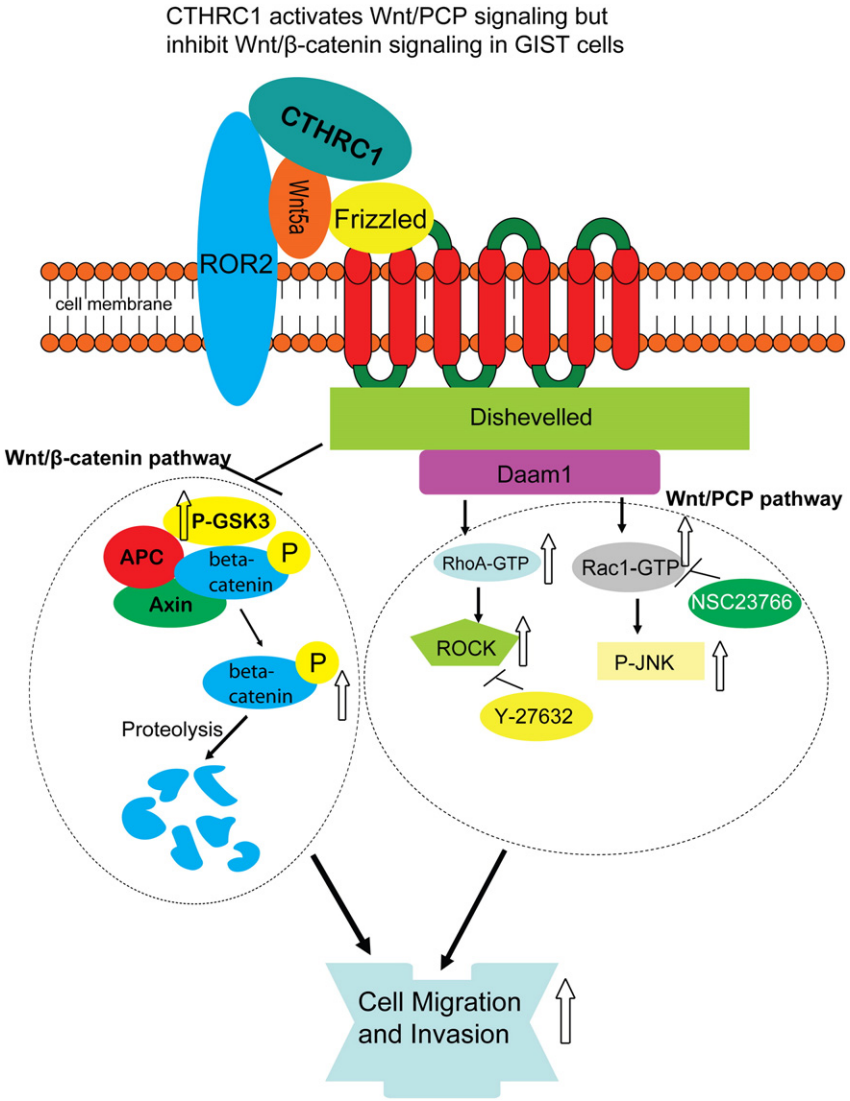

Figure 9. CTHRC1 induced cell signaling alteration and its related cell movement.

Although the functional roles of CTHRC1 in tumor cell invasion and metastasis have been well established, the underlying mechanisms of how CTHRC1 promotes cancer cell invasion remains unclear. It has been reported that CTHRC1 acts as a Wnt cofactor that selectively activates the PCP pathway in the inner ear developmental process [17]. In the present study, we showed that CTHRC1 promotes GIST cell invasion by activating Wnt/PCP signaling, which is supported by the following evidence. First, the luciferase reporter assay and western blotting showed that recombinant CTHRC1 protein activated the PCP pathway of Wnt signaling of primary GIST cells in a dose-dependent manner. Second, the pro-invasion activity of the rCTHRC1 protein was blocked by the neutralizing antibody of Wnt5a (a ligand for Wnt/PCP pathway [32,33]) and the inhibitors of Rac1 and ROCK (the downstream molecules of Wnt/PCP signaling [34,35]).

CTHRC1 promoted tumor cells migration by activating Rac1 and resulted in metastasis of pancreatic cancer [18]. The overexpression of *CTHRC1* promotes tumor invasion by activating RhoA in hepatocellular carcinoma [13]. Accordingly, we demonstrated the promoting effect of CTHRC1 on both RhoA and Rac1 in GIST cells. Moreover, we further verified that the pro-invasion activity of CTHRC1 in GIST cells was dependent on the Wnt5a/PCP-Rho axis by blocking the Wnt5a/PCP-Rho pathway with neutralizing antibodies and specific inhibitors. The noncanonical Wnt/PCP pathway transmits signaling from the cell-surface Frizzled receptor-coupled Wnt5a protein, via the Dvl-RhoA/Rac1-JNK-ATF2/c-Jun cascade [36-38], to the nucleus. Noncanonical Wnt/PCP signaling plays important roles in promoting cell migration [39] and formation of cell protrusions [40,41]. The small Rho GTPases Rac1, RhoA and Cdc42, are key executors of Wnt/PCP related cell migration [42,43]. RhoA controls the assembly of actin to generate contractile forces [44,45], while Rac1 and Cdc42 promote actin polymerization contributing to the formation of protrusive forces [46,47]. Therefore, the efficient cell movement requires synergistic actions of the three Rho GTPases [48-50]. In this study, we have shown that CTHRC1, a secreted protein, transduces outside-in signals through the Wnt/PCP pathway and coordinates the action of the three Rho GTPases to promote GIST cell migration and invasion.

Taken together, we have demonstrated that CTHRC1 expression level is closely correlated with risk grade of NIH classification

and prognosis of GIST, indicating that CTHRC1 served as a new predictor of recurrence risk and prognosis in post-operative GIST patients. Furthermore, we have shown that CTHRC1 promotes GIST cell migration and invasion by activating the Wnt/PCP-Rho signaling, suggesting that the CTHRC1- Wnt/PCP-Rho axis may be a new therapeutic target for interventions against GIST invasion and metastasis.

Acknowledgments

The study was supported by the National Science Foundation of China (81071738; 81101600, 81272743 and 81302094), Shanghai Health Bureau Youth Fund (2009Y110). ZGZ and HC were the principal investigator and supervised the implementation of the study. MZM wrote the protocols and, with CZ, XMY, ZZZ and HYY, analyzed the data and interpreted the findings. CZ and MZM were responsible for the collection of clinical data. HM had successfully isolated primary GIST cells from patients' tissues. MZM and CZ carried out the experiments involved in this article. HC, ZGZ, JRG, SLY and WXQ participated in critical revision of the manuscript for important intellectual content. All authors had full access to the primary data and the final analysis and approved the final version of the manuscript.

These authors declare no conflict of interest.

References

[1] Joensuu H, Hohenberger P, and Corless CL (2013). Gastrointestinal stromal tumour. *Lancet* **382**, 973–983.

[2] Yang H, Shen C, Zhang B, Chen H, Chen Z, and Chen J (2013). Expression and clinicopathological significance of CD9 in gastrointestinal stromal tumor. *J Korean Med Sci* **28**, 1443–1448.

[3] Terada T (2013). Smooth muscles and stem cells of embryonic guts express KIT, PDGFRRA, CD34 and many other stem cell antigens: suggestion that GIST arise from smooth muscles and gut stem cells. *Int J Clin Exp Pathol* **6**, 1038–1045.

[4] Simon S, Grabellus F, Ferrera L, Galietta L, Schwindenhammer B, Muhlenberg T, Taeger G, Eilers G, Treckmann J, and Breitenbuecher F, et al (2013). DOG1 regulates growth and IGFBP5 in gastrointestinal stromal tumors. *Cancer Res* **73**, 3661–3670.

[5] Hirano K, Shishido-Hara Y, Kitazawa A, Kojima K, Sumiishi A, Umino M, Kikuchi F, Sakamoto A, Fujioka Y, and Kamma H (2008). Expression of stem cell factor (SCF), a KIT ligand, in gastrointestinal stromal tumors (GISTs): a potential marker for tumor proliferation. *Pathol Res Pract* **204**, 799–807.

[6] Lv A, Li Z, Tian X, Guan X, Zhao M, Dong B, and Hao C (2013). SKP2 high expression, KIT exon 11 deletions, and gastrointestinal bleeding as predictors of poor prognosis in primary gastrointestinal stromal tumors. *PLoS One* **8**, e62951.

[7] Kubota D, Yoshida A, Tsuda H, Suehara Y, Okubo T, Saito T, Orita H, Sato K, Taguchi T, and Yao T, et al (2013). Gene expression network analysis of ETV1 reveals KCTD10 as a novel prognostic biomarker in gastrointestinal stromal tumor. *PLoS One* **8**, e73896.

[8] Shinomura Y, Kinoshita K, Tsutsui S, and Hirota S (2005). Pathophysiology, diagnosis, and treatment of gastrointestinal stromal tumors. *J Gastroenterol* **40**, 775–780.

[9] Joensuu H, Eriksson M, Sundby Hall K, Hartmann JT, Pink D, Schutte J, Ramadori G, Hohenberger P, Duyster J, and Al-Batran SE, et al (2012). One vs three years of adjuvant imatinib for operable gastrointestinal stromal tumor: a randomized trial. *JAMA* **307**, 1265–1272.

[10] Demetri GD, Reichardt P, Kang YK, Blay JY, Rutkowski P, Gelderblom H, Hohenberger P, Leahy M, von Mehren M, and Joensuu H, et al (2013). Efficacy and safety of regorafenib for advanced gastrointestinal stromal tumours after failure of imatinib and sunitinib (GRID): an international, multicentre, randomised, placebo-controlled, phase 3 trial. *Lancet* **381**, 295–302.

[11] Miettinen M and Lasota J (2001). Gastrointestinal stromal tumors–definition, clinical, histological, immunohistochemical, and molecular genetic features and differential diagnosis. *Virchows Arch* **438**, 1–12.

[12] Mucciarini C, Rossi G, Bertolini F, Valli R, Cirilli C, Rashid I, Marcheselli L, Luppi G, and Federico M (2007). Incidence and clinicopathologic features of gastrointestinal stromal tumors A population-based study. *BMC Cancer* **7**, 230.

[13] Chen YL, Wang TH, Hsu HC, Yuan RH, and Jeng YM (2013). Overexpression of CTHRC1 in Hepatocellular Carcinoma Promotes Tumor Invasion and Predicts Poor Prognosis. *PloS One* **8**, e70324.

[14] Lu P, Weaver VM, and Werb Z (2012). The extracellular matrix: a dynamic niche in cancer progression. *J Cell Biol* **196**, 395–406.

[15] Nguyen-Ngoc KV, Cheung KJ, Brenot A, Shamir ER, Gray RS, Hines WC, Yaswen P, Werb Z, and Ewald AJ (2012). ECM microenvironment regulates collective migration and local dissemination in normal and malignant mammary epithelium. *Proc Natl Acad Sci U S A* **109**, E2595-604.

[16] Pyagay P, Heroult M, Wang Q, Lehnert W, Belden J, Liaw L, Friesel RE, and Lindner V (2005). Collagen triple helix repeat containing 1, a novel secreted protein in injured and diseased arteries, inhibits collagen expression and promotes cell migration. *Circ Res* **96**, 261–268.

[17] Yamamoto S, Nishimura O, Misaki K, Nishita M, Minami Y, Yonemura S, Tarui H, and Sasaki H (2008). Cthrc1 selectively activates the planar cell polarity pathway of Wnt signaling by stabilizing the Wnt-receptor complex. *Dev Cell* **15**, 23–36.

[18] Park EH, Kim S, Jo JY, Kim SJ, Hwang Y, Kim JM, Song SY, Lee DK, and Koh SS (2013). Collagen triple helix repeat containing-1 promotes pancreatic cancer progression by regulating migration and adhesion of tumor cells. *Carcinogenesis* **34**, 694–702.

[19] Wang P, Wang YC, Chen XY, Shen ZY, Cao H, Zhang YJ, Yu J, Zhu JD, Lu YY, and Fang JY (2012). CTHRC1 is upregulated by promoter demethylation and transforming growth factor-beta1 and may be associated with metastasis in human gastric cancer. *Cancer Sci* **103**, 1327–1333.

[20] Tan F, Liu F, Liu H, Hu Y, Liu D, and Li G (2013). CTHRC1 is associated with peritoneal carcinomatosis in colorectal cancer: a new predictor for prognosis. *Med Oncol* **30**, 473.

[21] Joensuu H (2008). Risk stratification of patients diagnosed with gastrointestinal stromal tumor. *Hum Pathol* **39**, 1411–1419.

[22] Rutkowski P, Bylina E, Wozniak A, Nowecki ZI, Osuch C, Matlok M, Switaj T, Michej W, Wronski M, and Gluszek S, et al (2011). Validation of the Joensuu risk criteria for primary resectable gastrointestinal stromal tumour - the impact of tumour rupture on patient outcomes. *Eur J Surg Oncol* **37**, 890–896.

[23] Zhang ZG, Lambert C, Servotte S, Chometon G, Eckes B, Krieg T, Lapiere C, Nusgens B, and Aumailley M (2006). Effects of constitutively active GTPases on fibroblast behavior. *Cell Mol Life Sci* **63**, 82–91.

[24] Steigen SE and Eide TJ (2009). Gastrointestinal stromal tumors (GISTs): a review. *APMIS* **117**, 73–86.

[25] Pidhorecky I, Cheney RT, Kraybill WG, and Gibbs JF (2000). Gastrointestinal stromal tumors: current diagnosis, biologic behavior, and management. *Ann Surg Oncol* **7**, 705–712.

[26] Lee EJ, Kang G, Kang SW, Jang KT, Lee J, Park JO, Park CK, Sohn TS, Kim S, and Kim KM (2013). GSTT1 copy number gain and ZNF overexpression are predictors of poor response to imatinib in gastrointestinal stromal tumors. *PLoS One* **8**, e77219.

[27] Fletcher CD, Berman JJ, Corless C, Gorstein F, Lasota J, Longley BJ, Miettinen M, O'Leary TJ, Remotti H, and Rubin BP, et al (2002). Diagnosis of gastrointestinal stromal tumors: A consensus approach. *Hum Pathol* **33**, 459–465.

[28] Fletcher CD, Berman JJ, Corless C, Gorstein F, Lasota J, Longley BJ, Miettinen M, O'Leary TJ, Remotti H, and Rubin BP, et al (2002). Diagnosis of gastrointestinal stromal tumors: a consensus approach. *Int J Surg Pathol* **10**, 81–89.

[29] Miao CG, Yang YY, He X, Li XF, Huang C, Huang Y, Zhang L, Lv XW, Jin Y, and Li J (2013). Wnt signaling pathway in rheumatoid arthritis, with special emphasis on the different roles in synovial inflammation and bone remodeling. *Cell Signal* **25**, 2069–2078.

[30] Rabelo Fde S, da Mota LM, Lima RA, Lima FA, Barra GB, de Carvalho JF, and Amato AA (2010). The Wnt signaling pathway and rheumatoid arthritis. *Autoimmun Rev* **9**, 207–210.

[31] Spano D and Zollo M (2012). Tumor microenvironment: a main actor in the metastasis process. *Clin Exp Metastasis* **29**, 381–395.

[32] Niehrs C (2012). The complex world of WNT receptor signalling. *Nat Rev Mol Cell Biol* **13**, 767–779.

[33] Zeller J, Turbiak AJ, Powelson IA, Lee S, Sun D, Showalter HD, and Fearon ER (2013). Investigation of 3-aryl-pyrimido[5,4-e][1,2,4]triazine-5,7-diones as small

molecule antagonists of beta-catenin/TCF transcription. *Bioorg Med Chem Lett* **23**, 5814–5820.

[34] Choi SS, Witek RP, Yang L, Omenetti A, Syn WK, Moylan CA, Jung Y, Karaca GF, Teaberry VS, and Pereira TA, et al (2010). Activation of Rac1 promotes hedgehog-mediated acquisition of the myofibroblastic phenotype in rat and human hepatic stellate cells. *Hepatology* **52**, 278–290.

[35] Huang X, McGann JC, Liu BY, Hannoush RN, Lill JR, Pham V, Newton K, Kakunda M, Liu J, and Yu C, et al (2013). Phosphorylation of Dishevelled by protein kinase RIPK4 regulates Wnt signaling. *Science* **339**, 1441–1445.

[36] Yuan Y, Niu CC, Deng G, Li ZQ, Pan J, Zhao C, Yang ZL, and Si WK (2011). The Wnt5a/Ror2 noncanonical signaling pathway inhibits canonical Wnt signaling in K562 cells. *Int J Mol Med* **27**, 63–69.

[37] Wada H and Okamoto H (2009). Roles of noncanonical Wnt/PCP pathway genes in neuronal migration and neurulation in zebrafish. *Zebrafish* **6**, 3–8.

[38] Gao B (2012). Wnt regulation of planar cell polarity (PCP). *Curr Top Dev Biol* **101**, 263–295.

[39] Miyoshi H, Ajima R, Luo CT, Yamaguchi TP, and Stappenbeck TS (2012). Wnt5a potentiates TGF-beta signaling to promote colonic crypt regeneration after tissue injury. *Science* **338**, 108–113.

[40] Katoh M (2005). WNT/PCP signaling pathway and human cancer (review). *Oncol Rep* **14**, 1583–1588.

[41] Otey C, Goicoechea S, and Garcia-Mata R (2009). Roles of the small GTPases RhoA and Rac1 in cell behavior. *F1000 Biol Rep* **1**, 4.

[42] Maeda K, Kobayashi Y, Udagawa N, Uehara S, Ishihara A, Mizoguchi T, Kikuchi Y, Takada I, Kato S, and Kani S, et al (2012). Wnt5a-Ror2 signaling between osteoblast-lineage cells and osteoclast precursors enhances osteoclastogenesis. *Nat Med* **18**, 405–412.

[43] Kamai T, Yamanishi T, Shirataki H, Takagi K, Asami H, Ito Y, and Yoshida K (2004). Overexpression of RhoA, Rac1, and Cdc42 GTPases is associated with progression in testicular cancer. *Clin Cancer Res* **10**, 4799–4805.

[44] Deakin NO, Ballestrem C, and Turner CE (2012). Paxillin and Hic-5 interaction with vinculin is differentially regulated by Rac1 and RhoA. *PLoS One* **7**, e37990.

[45] Chauhan BK, Lou M, Zheng Y, and Lang RA (2011). Balanced Rac1 and RhoA activities regulate cell shape and drive invagination morphogenesis in epithelia. *Proc Natl Acad Sci U S A* **108**, 18289–18294.

[46] Hill CS, Wynne J, and Treisman R (1995). The Rho family GTPases RhoA, Rac1, and CDC42Hs regulate transcriptional activation by SRF. *Cell* **81**, 1159–1170.

[47] El-Sibai M, Pertz O, Pang H, Yip SC, Lorenz M, Symons M, Condeelis JS, Hahn KM, and Backer JM (2008). RhoA/ROCK-mediated switching between Cdc42- and Rac1-dependent protrusion in MTLn3 carcinoma cells. *Exp Cell Res* **314**, 1540–1552.

[48] Nethe M and Hordijk PL (2010). The role of ubiquitylation and degradation in RhoGTPase signalling. *J Cell Sci* **123**, 4011–4018.

[49] Patel S, Takagi KI, Suzuki J, Imaizumi A, Kimura T, Mason RM, Kamimura T, and Zhang Z (2005). RhoGTPase activation is a key step in renal epithelial mesenchymal transdifferentiation. *J Am Soc Nephrol* **16**, 1977–1984.

[50] Bravo-Cordero JJ, Moshfegh Y, Condeelis J, and Hodgson L (2013). Live cell imaging of RhoGTPase biosensors in tumor cells. *Methods Mol Biol* **1046**, 359–370.

Supplementary materials

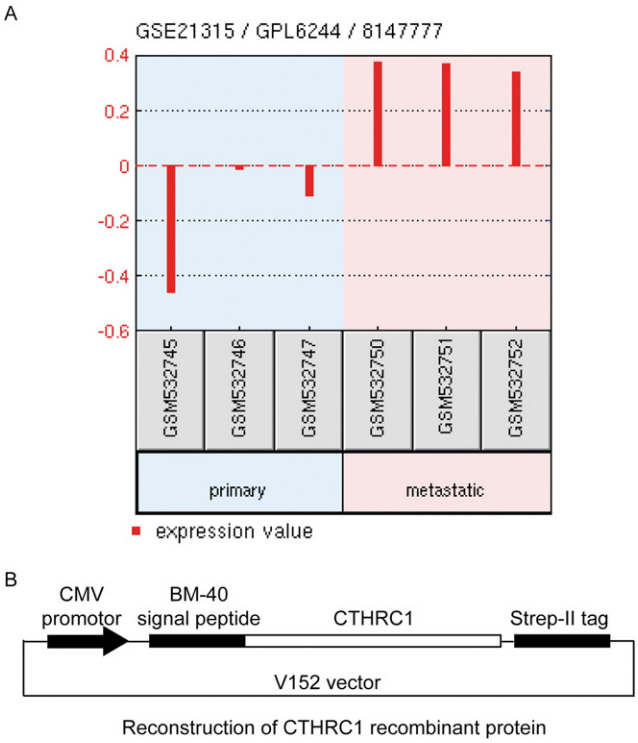

Figure W1. (A) Analysis of *CTHRC1* differential expression in metastatic GIST and primary GIST based on data from GEO Database (GSE21315). (B) Schematic diagram of V152 vector which was used to reconstruct *CTHRC1*-StrepII recombinant plasmid.

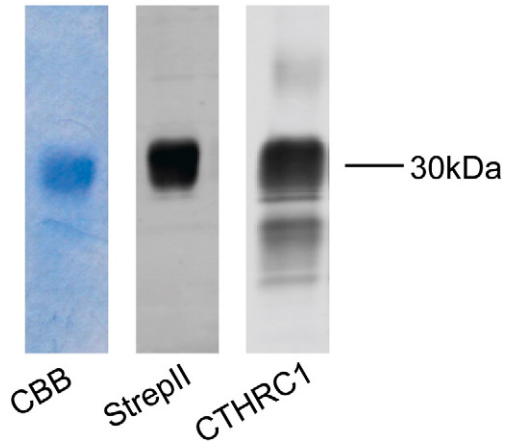

Figure W2. Verification of affinity purified CTHRC1 protein by Coomassie Brilliant Blue staining and Western blotting.

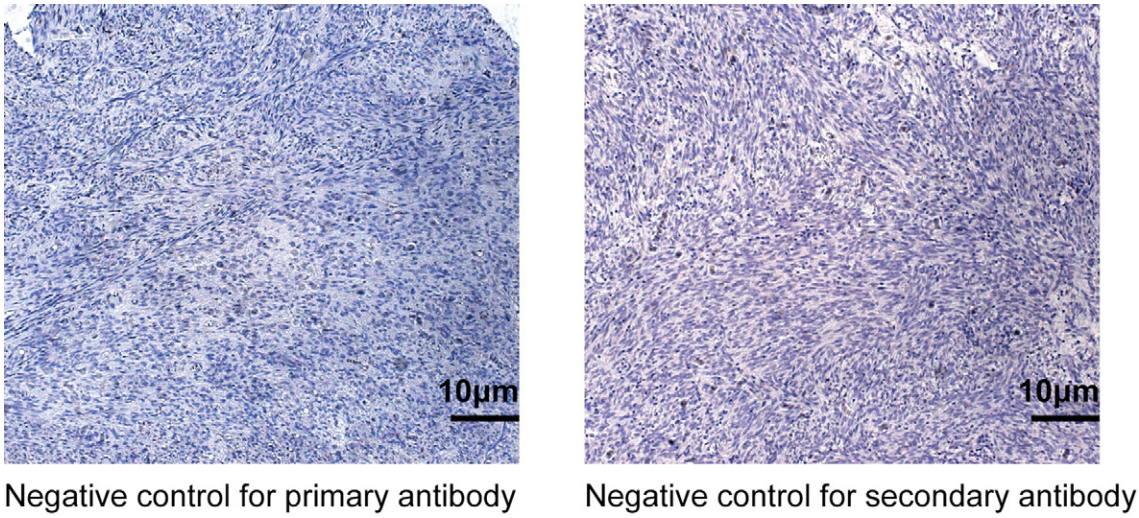

Figure W3. Negative controls for primary and secondary antibodies in GIST TMA immunohistochemistry staining assay (original magnification: 100×).

Table W1. ANOVA analysis (post-hoc testing) for statistics of figures.

Multiple Comparisons						
(I) 1 = low risk, 2 = intermediate risk, 3 = high risk	(J) 1 = low risk, 2 = intermediate risk, 3 = high risk	Mean Difference (I-J)	Std. Error	Sig.	95% Confidence Interval	
					Lower Bound	Upper Bound
Figure 1A						
1	2	−1.53243*	.57014	.031	−2.9405	-.1244
	3	−1.47190*	.58777	.046	−2.9235	-.0203
2	1	1.53243*	.57014	.031	.1244	2.9405
	3	.06053	.62280	.995	−1.4776	1.5986
3	1	1.47190*	.58777	.046	.0203	2.9235
	2	-.06053	.62280	.995	−1.5986	1.4776
VAR00001						
Tukey HSD						

Multiple Comparisons

(I) concentration	(J) concentration	Mean Difference (I-J)	Std. Error	Sig.	95% Confidence Interval	
					Lower Bound	Upper Bound
Figure 3B						
Day0						
0	1	-.0040000	.0094810	.973	-.034361	.026361
	20	-.0160000	.0094810	.389	-.046361	.014361
	50	-.0013333	.0094810	.999	-.031695	.029028
1	0	.0040000	.0094810	.973	-.026361	.034361
	20	-.0120000	.0094810	.607	-.042361	.018361
	50	.0026667	.0094810	.992	-.027695	.033028
20	0	.0160000	.0094810	.389	-.014361	.046361
	1	.0120000	.0094810	.607	-.018361	.042361
	50	.0146667	.0094810	.456	-.015695	.045028
50	0	.0013333	.0094810	.999	-.029028	.031695
	1	-.0026667	.0094810	.992	-.033028	.027695
	20	-.0146667	.0094810	.456	-.045028	.015695
VAR00001						
Tukey HSD						

Table W1. (*continued*)

Multiple Comparisons

(I) concentration	(J) concentration	Mean Difference (I-J)	Std. Error	Sig.	95% Confidence Interval	
					Lower Bound	Upper Bound
Figure 3B Day1						
0	1	.0023333	.0055578	.973	-.015465	.020131
	20	-.0216667*	.0055578	.019	-.039465	-.003869
	50	-.0230000*	.0055578	.014	-.040798	-.005202
1	0	-.0023333	.0055578	.973	-.020131	.015465
	20	-.0240000*	.0055578	.011	-.041798	-.006202
	50	-.0253333*	.0055578	.008	-.043131	-.007535
20	0	.0216667*	.0055578	.019	.003869	.039465
	1	.0240000*	.0055578	.011	.006202	.041798
	50	-.0013333	.0055578	.995	-.019131	.016465
50	0	.0230000*	.0055578	.014	.005202	.040798
	1	.0253333*	.0055578	.008	.007535	.043131
	20	.0013333	.0055578	.995	-.016465	.019131
VAR00001 Tukey HSD						

Multiple Comparisons

(I) concentration	(J) concentration	Mean Difference (I-J)	Std. Error	Sig.	95% Confidence Interval	
					Lower Bound	Upper Bound
Figure 3B Day2						
0	1	-.0596667*	.0133083	.009	-.102285	-.017049
	20	-.0253333	.0133083	.299	-.067951	.017285
	50	-.0746667*	.0133083	.002	-.117285	-.032049
1	0	.0596667*	.0133083	.009	.017049	.102285
	20	.0343333	.0133083	.120	-.008285	.076951
	50	-.0150000	.0133083	.684	-.057618	.027618
20	0	.0253333	.0133083	.299	-.017285	.067951
	1	-.0343333	.0133083	.120	-.076951	.008285
	50	-.0493333*	.0133083	.025	-.091951	-.006715
50	0	.0746667*	.0133083	.002	.032049	.117285
	1	.0150000	.0133083	.684	-.027618	.057618
	20	.0493333*	.0133083	.025	.006715	.091951
VAR00001 Tukey HSD						

Multiple Comparisons

(I) concentration	(J) concentration	Mean Difference (I-J)	Std. Error	Sig.	95% Confidence Interval	
					Lower Bound	Upper Bound
Figure 3B Day3						
0	1	-.0046667	.0051962	.806	-.021307	.011973
	20	-.0223333*	.0051962	.011	-.038973	-.005693
	50	-.0283333*	.0051962	.003	-.044973	-.011693
1	0	.0046667	.0051962	.806	-.011973	.021307
	20	-.0176667*	.0051962	.038	-.034307	-.001027
	50	-.0236667*	.0051962	.008	-.040307	-.007027
20	0	.0223333*	.0051962	.011	.005693	.038973
	1	.0176667*	.0051962	.038	.001027	.034307
	50	-.0060000	.0051962	.669	-.022640	.010640
50	0	.0283333*	.0051962	.003	.011693	.044973
	1	.0236667*	.0051962	.008	.007027	.040307
	20	.0060000	.0051962	.669	-.010640	.022640
VAR00001 Tukey HSD						

Table W1. (*continued*)

Multiple Comparisons

(I) concentration	(J) concentration	Mean Difference (I-J)	Std. Error	Sig.	95% Confidence Interval	
					Lower Bound	Upper Bound
Figure 3B Day4						
0	1	-.0030000	.0072111	.974	-.026092	.020092
	20	.0173333	.0072111	.154	-.005759	.040426
	50	-.0753333*	.0072111	.000	-.098426	-.052241
1	0	.0030000	.0072111	.974	-.020092	.026092
	20	.0203333	.0072111	.086	-.002759	.043426
	50	-.0723333*	.0072111	.000	-.095426	-.049241
20	0	-.0173333	.0072111	.154	-.040426	.005759
	1	-.0203333	.0072111	.086	-.043426	.002759
	50	-.0926667*	.0072111	.000	-.115759	-.069574
50	0	.0753333*	.0072111	.000	.052241	.098426
	1	.0723333*	.0072111	.000	.049241	.095426
	20	.0926667*	.0072111	.000	.069574	.115759
VAR00001 Tukey HSD						

Multiple Comparisons

(I) concentration	(J) concentration	Mean Difference (I-J)	Std. Error	Sig.	95% Confidence Interval	
					Lower Bound	Upper Bound
Figure 3B Day5						
0	1	.0146667	.0078916	.316	-.010605	.039938
	20	-.0660000*	.0078916	.000	-.091272	-.040728
	50	-.0893333*	.0078916	.000	-.114605	-.064062
1	0	-.0146667	.0078916	.316	-.039938	.010605
	20	-.0806667*	.0078916	.000	-.105938	-.055395
	50	-.1040000*	.0078916	.000	-.129272	-.078728
20	0	.0660000*	.0078916	.000	.040728	.091272
	1	.0806667*	.0078916	.000	.055395	.105938
	50	-.0233333	.0078916	.071	-.048605	.001938
50	0	.0893333*	.0078916	.000	.064062	.114605
	1	.1040000*	.0078916	.000	.078728	.129272
	20	.0233333	.0078916	.071	-.001938	.048605
VAR00001 Tukey HSD						

Multiple Comparisons

(I) concentration	(J) concentration	Mean Difference (I-J)	Std. Error	Sig.	95% Confidence Interval	
					Lower Bound	Upper Bound
Figure 3B Day6						
0	1	-.0046667	.0106797	.970	-.038867	.029533
	20	-.0750000*	.0106797	.001	-.109200	-.040800
	50	-.1590000*	.0106797	.000	-.193200	-.124800
1	0	.0046667	.0106797	.970	-.029533	.038867
	20	-.0703333*	.0106797	.001	-.104533	-.036133
	50	-.1543333*	.0106797	.000	-.188533	-.120133
20	0	.0750000*	.0106797	.001	.040800	.109200
	1	.0703333*	.0106797	.001	.036133	.104533
	50	-.0840000*	.0106797	.000	-.118200	-.049800
50	0	.1590000*	.0106797	.000	.124800	.193200
	1	.1543333*	.0106797	.000	.120133	.188533
	20	.0840000*	.0106797	.000	.049800	.118200
VAR00001 Tukey HSD						

Table W1. (*continued*)

Multiple Comparisons

(I) VAR00002	(J) VAR00002	Mean Difference (I-J)	Std. Error	Sig.	95% Confidence Interval	
					Lower Bound	Upper Bound
Figure 3C						
0	1	−6.50000*	1.69558	.005	−11.2458	−1.7542
	20	−55.50000*	1.69558	.000	−60.2458	−50.7542
	50	−69.16667*	1.69558	.000	−73.9125	−64.4208
1	0	6.50000*	1.69558	.005	1.7542	11.2458
	20	−49.00000*	1.69558	.000	−53.7458	−44.2542
	50	−62.66667*	1.69558	.000	−67.4125	−57.9208
20	0	55.50000*	1.69558	.000	50.7542	60.2458
	1	49.00000*	1.69558	.000	44.2542	53.7458
	50	−13.66667*	1.69558	.000	−18.4125	−8.9208
50	0	69.16667*	1.69558	.000	64.4208	73.9125
	1	62.66667*	1.69558	.000	57.9208	67.4125
	20	13.66667*	1.69558	.000	8.9208	18.4125
VAR00001						
Tukey HSD						

Multiple Comparisons

(I) concentration	(J) concentration	Mean Difference (I-J)	Std. Error	Sig.	95% Confidence Interval	
					Lower Bound	Upper Bound
Figure 3D						
0	1	−23.66667*	3.28549	.000	−32.8625	−14.4708
	20	−55.50000*	3.28549	.000	−64.6959	−46.3041
	50	−72.16667*	3.28549	.000	−81.3625	−62.9708
1	0	23.66667*	3.28549	.000	14.4708	32.8625
	20	−31.83333*	3.28549	.000	−41.0292	−22.6375
	50	−48.50000*	3.28549	.000	−57.6959	−39.3041
20	0	55.50000*	3.28549	.000	46.3041	64.6959
	1	31.83333*	3.28549	.000	22.6375	41.0292
	50	−16.66667*	3.28549	.000	−25.8625	−7.4708
50	0	72.16667*	3.28549	.000	62.9708	81.3625
	1	48.50000*	3.28549	.000	39.3041	57.6959
	20	16.66667*	3.28549	.000	7.4708	25.8625
VAR00001						
Tukey HSD						

Multiple Comparisons

(I) VAR00002	(J) VAR00002	Mean Difference (I-J)	Std. Error	Sig.	95% Confidence Interval	
					Lower Bound	Upper Bound
Figure 4A (Mutant TCF)						
0	1	-.01200	.02143	.941	-.0806	.0566
	20	-.02933	.02143	.550	-.0980	.0393
	50	-.04333	.02143	.257	-.1120	.0253
1	0	.01200	.02143	.941	-.0566	.0806
	20	-.01733	.02143	.849	-.0860	.0513
	50	-.03133	.02143	.500	-.1000	.0373
20	0	.02933	.02143	.550	-.0393	.0980
	1	.01733	.02143	.849	-.0513	.0860
	50	-.01400	.02143	.911	-.0826	.0546
50	0	.04333	.02143	.257	-.0253	.1120
	1	.03133	.02143	.500	-.0373	.1000
	20	.01400	.02143	.911	-.0546	.0826
VAR00001						
Tukey HSD						

Table W1. (*continued*)

Multiple Comparisons

(I) VAR00002	(J) VAR00002	Mean Difference (I-J)	Std. Error	Sig.	95% Confidence Interval	
					Lower Bound	Upper Bound
Figure 4A (TCF)						
0	1	.19167 *	.02076	.000	.1252	.2582
	20	.30900 *	.02076	.000	.2425	.3755
	50	.46600 *	.02076	.000	.3995	.5325
1	0	-.19167 *	.02076	.000	-.2582	-.1252
	20	.11733 *	.02076	.002	.0508	.1838
	50	.27433 *	.02076	.000	.2078	.3408
20	0	-.30900 *	.02076	.000	-.3755	-.2425
	1	-.11733 *	.02076	.002	-.1838	-.0508
	50	.15700 *	.02076	.000	.0905	.2235
50	0	-.46600 *	.02076	.000	-.5325	-.3995
	1	-.27433 *	.02076	.000	-.3408	-.2078
	20	-.15700 *	.02076	.000	-.2235	-.0905

VAR00001
Tukey HSD

Multiple Comparisons

(I) VAR00002	(J) VAR00002	Mean Difference (I-J)	Std. Error	Sig.	95% Confidence Interval	
					Lower Bound	Upper Bound
Figure 4B						
0	1	−1.92467 *	.41532	.007	−3.2547	-.5947
	20	−2.50733 *	.41532	.001	−3.8373	−1.1773
	50	−6.96000 *	.41532	.000	−8.2900	−5.6300
1	0	1.92467 *	.41532	.007	.5947	3.2547
	20	-.58267	.41532	.531	−1.9127	.7473
	50	−5.03533 *	.41532	.000	−6.3653	−3.7053
20	0	2.50733 *	.41532	.001	1.1773	3.8373
	1	.58267	.41532	.531	-.7473	1.9127
	50	−4.45267 *	.41532	.000	−5.7827	−3.1227
50	0	6.96000 *	.41532	.000	5.6300	8.2900
	1	5.03533 *	.41532	.000	3.7053	6.3653
	20	4.45267 *	.41532	.000	3.1227	5.7827

VAR00001
Tukey HSD

Multiple Comparisons

(I) 1 = 0nm, 2 = 20nm, 3 = 0nm+Wnt5a mAb, 4 = 20nm+Wnt5a mAb	(J) 1 = 0nm, 2 = 20nm, 3 = 0nm+Wnt5a mAb, 4 = 20nm+Wnt5a mAb	Mean Difference (I-J)	Std. Error	Sig.	95% Confidence Interval	
					Lower Bound	Upper Bound
Figure 4C						
1	2	.33467 *	.03334	.000	.2279	.4414
	3	.04400	.03334	.577	-.0628	.1508
	4	.16100 *	.03334	.006	.0542	.2678
2	1	-.33467 *	.03334	.000	-.4414	-.2279
	3	-.29067 *	.03334	.000	-.3974	-.1839
	4	-.17367 *	.03334	.004	-.2804	-.0669
3	1	-.04400	.03334	.577	-.1508	.0628
	2	.29067 *	.03334	.000	.1839	.3974
	4	.11700 *	.03334	.033	.0102	.2238
4	1	-.16100 *	.03334	.006	-.2678	-.0542
	2	.17367 *	.03334	.004	.0669	.2804
	3	-.11700 *	.03334	.033	-.2238	-.0102

VAR00001
Tukey HSD

Table W1. (*continued*)

Multiple Comparisons

(I) VAR00002	(J) VAR00002	Mean Difference (I-J)	Std. Error	Sig.	95% Confidence Interval	
					Lower Bound	Upper Bound
Figure 4D						
1	2	−2.75433*	.27391	.000	−3.6315	−1.8772
	3	1.07233*	.27391	.019	.1952	1.9495
	4	-.32100	.27391	.659	−1.1981	.5561
2	1	2.75433*	.27391	.000	1.8772	3.6315
	3	3.82667*	.27391	.000	2.9495	4.7038
	4	2.43333*	.27391	.000	1.5562	3.3105
3	1	−1.07233*	.27391	.019	−1.9495	-.1952
	2	−3.82667*	.27391	.000	−4.7038	−2.9495
	4	−1.39333*	.27391	.004	−2.2705	-.5162
4	1	.32100	.27391	.659	-.5561	1.1981
	2	−2.43333*	.27391	.000	−3.3105	−1.5562
	3	1.39333*	.27391	.004	.5162	2.2705

VAR00001
Tukey HSD

Multiple Comparisons

(I) 1 = NC, 2 = +Wnt3a, 3 = +Wnt3a mAb, 4 = Wnt3a+Wnt3a mAb	(J) 1 = NC, 2 = +Wnt3a, 3 = +Wnt3a mAb, 4 = Wnt3a+Wnt3a mAb	Mean Difference (I-J)	Std. Error	Sig.	95% Confidence Interval	
					Lower Bound	Upper Bound
Figure 4E						
1	2	-.47433*	.04523	.000	-.6192	-.3295
	3	.17733*	.04523	.019	.0325	.3222
	4	.16567*	.04523	.026	.0208	.3105
2	1	.47433*	.04523	.000	.3295	.6192
	3	.65167*	.04523	.000	.5068	.7965
	4	.64000*	.04523	.000	.4951	.7849
3	1	-.17733*	.04523	.019	-.3222	-.0325
	2	-.65167*	.04523	.000	-.7965	-.5068
	4	-.01167	.04523	.994	-.1565	.1332
4	1	-.16567*	.04523	.026	-.3105	-.0208
	2	-.64000*	.04523	.000	-.7849	-.4951
	3	.01167	.04523	.994	-.1332	.1565

VAR00001
Tukey HSD

Multiple Comparisons

(I) 1 = NC, 2 = +Wnt5a, 3 = +Wnt5a mAb, 4 = Wnt5a+Wnt5a mAb	(J) 1 = NC, 2 = +Wnt5a, 3 = +Wnt5a mAb, 4 = Wnt5a+Wnt5a mAb	Mean Difference (I-J)	Std. Error	Sig.	95% Confidence Interval	
					Lower Bound	Upper Bound
Figure 4F						
1	2	−3.02767*	.20239	.000	−3.6758	−2.3795
	3	1.02867*	.20239	.004	.3805	1.6768
	4	-.17100	.20239	.832	-.8191	.4771
2	1	3.02767*	.20239	.000	2.3795	3.6758
	3	4.05633*	.20239	.000	3.4082	4.7045
	4	2.85667*	.20239	.000	2.2085	3.5048
3	1	−1.02867*	.20239	.004	−1.6768	-.3805
	2	−4.05633*	.20239	.000	−4.7045	−3.4082
	4	−1.19967*	.20239	.002	−1.8478	-.5515
4	1	.17100	.20239	.832	-.4771	.8191
	2	−2.85667*	.20239	.000	−3.5048	−2.2085
	3	1.19967*	.20239	.002	.5515	1.8478

VAR00001
Tukey HSD

Table W1. (*continued*)

Multiple Comparisons

(I) VAR00002	(J) VAR00002	Mean Difference (I-J)	Std. Error	Sig.	95% Confidence Interval	
					Lower Bound	Upper Bound
Figure 5B						
0	5	-.58300*	.05290	.000	-.7571	-.4089
	10	-.12600	.05290	.197	-.3001	.0481
	30	-.40433*	.05290	.000	-.5784	-.2302
	60	-.13600	.05290	.150	-.3101	.0381
5	0	.58300*	.05290	.000	.4089	.7571
	10	.45700*	.05290	.000	.2829	.6311
	30	.17867*	.05290	.044	.0046	.3528
	60	.44700*	.05290	.000	.2729	.6211
10	0	.12600	.05290	.197	-.0481	.3001
	5	-.45700*	.05290	.000	-.6311	-.2829
	30	-.27833*	.05290	.003	-.4524	-.1042
	60	-.01000	.05290	1.000	-.1841	.1641
30	0	.40433*	.05290	.000	.2302	.5784
	5	-.17867*	.05290	.044	-.3528	-.0046
	10	.27833*	.05290	.003	.1042	.4524
	60	.26833*	.05290	.003	.0942	.4424
60	0	.13600	.05290	.150	-.0381	.3101
	5	-.44700*	.05290	.000	-.6211	-.2729
	10	.01000	.05290	1.000	-.1641	.1841
	30	-.26833*	.05290	.003	-.4424	-.0942

VAR00001
Tukey HSD

Multiple Comparisons

(I) VAR00002	(J) VAR00002	Mean Difference (I-J)	Std. Error	Sig.	95% Confidence Interval	
					Lower Bound	Upper Bound
Figure 5C						
0	5	-.20667*	.01588	.000	-.2589	-.1544
	10	-.39767*	.01588	.000	-.4499	-.3454
	30	-.52167*	.01588	.000	-.5739	-.4694
	60	-.53733*	.01588	.000	-.5896	-.4851
5	0	.20667*	.01588	.000	.1544	.2589
	10	-.19100*	.01588	.000	-.2433	-.1387
	30	-.31500*	.01588	.000	-.3673	-.2627
	60	-.33067*	.01588	.000	-.3829	-.2784
10	0	.39767*	.01588	.000	.3454	.4499
	5	.19100*	.01588	.000	.1387	.2433
	30	-.12400*	.01588	.000	-.1763	-.0717
	60	-.13967*	.01588	.000	-.1919	-.0874
30	0	.52167*	.01588	.000	.4694	.5739
	5	.31500*	.01588	.000	.2627	.3673
	10	.12400*	.01588	.000	.0717	.1763
	60	-.01567	.01588	.855	-.0679	.0366
60	0	.53733*	.01588	.000	.4851	.5896
	5	.33067*	.01588	.000	.2784	.3829
	10	.13967*	.01588	.000	.0874	.1919
	30	.01567	.01588	.855	-.0366	.0679

VAR00001
Tukey HSD

Multiple Comparisons

(I) time	(J) time	Mean Difference (I-J)	Std. Error	Sig.	95% Confidence Interval	
					Lower Bound	Upper Bound
Figure 5D						
0	5	.03000	.03961	.937	-.1004	.1604
	10	-.01000	.03961	.999	-.1404	.1204
	30	.00667	.03961	1.000	-.1237	.1370
	60	-.02333	.03961	.974	-.1537	.1070
5	0	-.03000	.03961	.937	-.1604	.1004
	10	-.04000	.03961	.845	-.1704	.0904
	30	-.02333	.03961	.974	-.1537	.1070
	60	-.05333	.03961	.671	-.1837	.0770

Table W1. (*continued*)

10	0	.01000	.03961	.999	-.1204	.1404
	5	.04000	.03961	.845	-.0904	.1704
	30	.01667	.03961	.992	-.1137	.1470
	60	-.01333	.03961	.997	-.1437	.1170
30	0	-.00667	.03961	1.000	-.1370	.1237
	5	.02333	.03961	.974	-.1070	.1537
	10	-.01667	.03961	.992	-.1470	.1137
	60	-.03000	.03961	.937	-.1604	.1004
60	0	.02333	.03961	.974	-.1070	.1537
	5	.05333	.03961	.671	-.0770	.1837
	10	.01333	.03961	.997	-.1170	.1437
	30	.03000	.03961	.937	-.1004	.1604

VAR00001
Tukey HSD

Multiple Comparisons

(I) VAR00002	(J) VAR00002	Mean Difference (I-J)	Std. Error	Sig.	95% Confidence Interval	
					Lower Bound	Upper Bound
Figure 5E						
0	1	-.11033*	.02696	.015	-.1967	-.0240
	20	-.32633*	.02696	.000	-.4127	-.2400
	50	-.47333*	.02696	.000	-.5597	-.3870
1	0	.11033*	.02696	.015	.0240	.1967
	20	-.21600*	.02696	.000	-.3023	-.1297
	50	-.36300*	.02696	.000	-.4493	-.2767
20	0	.32633*	.02696	.000	.2400	.4127
	1	.21600*	.02696	.000	.1297	.3023
	50	-.14700*	.02696	.003	-.2333	-.0607
50	0	.47333*	.02696	.000	.3870	.5597
	1	.36300*	.02696	.000	.2767	.4493
	20	.14700*	.02696	.003	.0607	.2333

VAR00001
Tukey HSD

Multiple Comparisons

(I) VAR00002	(J) VAR00002	Mean Difference (I-J)	Std. Error	Sig.	95% Confidence Interval	
					Lower Bound	Upper Bound
Figure 5F						
0	1	-.15167*	.01790	.000	-.2090	-.0943
	20	-.39267*	.01790	.000	-.4500	-.3353
	50	-.51900*	.01790	.000	-.5763	-.4617
1	0	.15167*	.01790	.000	.0943	.2090
	20	-.24100*	.01790	.000	-.2983	-.1837
	50	-.36733*	.01790	.000	-.4247	-.3100
20	0	.39267*	.01790	.000	.3353	.4500
	1	.24100*	.01790	.000	.1837	.2983
	50	-.12633*	.01790	.000	-.1837	-.0690
50	0	.51900*	.01790	.000	.4617	.5763
	1	.36733*	.01790	.000	.3100	.4247
	20	.12633*	.01790	.000	.0690	.1837

VAR00001
Tukey HSD

Multiple Comparisons

(I) VAR00002	(J) VAR00002	Mean Difference (I-J)	Std. Error	Sig.	95% Confidence Interval	
					Lower Bound	Upper Bound
Figure 6C						
0	5	-.08967*	.02012	.008	-.1559	-.0234
	10	-.37167*	.02012	.000	-.4379	-.3054
	30	-.56933*	.02012	.000	-.6356	-.5031
	60	-.74133*	.02012	.000	-.8076	-.6751
5	0	.08967*	.02012	.008	.0234	.1559
	10	-.28200*	.02012	.000	-.3482	-.2158
	30	-.47967*	.02012	.000	-.5459	-.4134
	60	-.65167*	.02012	.000	-.7179	-.5854

Table W1. (*continued*)

10	0	.37167 *	.02012	.000	.3054	.4379
	5	.28200 *	.02012	.000	.2158	.3482
	30	-.19767 *	.02012	.000	-.2639	-.1314
	60	-.36967 *	.02012	.000	-.4359	-.3034
30	0	.56933 *	.02012	.000	.5031	.6356
	5	.47967 *	.02012	.000	.4134	.5459
	10	.19767 *	.02012	.000	.1314	.2639
	60	-.17200 *	.02012	.000	-.2382	-.1058
60	0	.74133 *	.02012	.000	.6751	.8076
	5	.65167 *	.02012	.000	.5854	.7179
	10	.36967 *	.02012	.000	.3034	.4359
	30	.17200 *	.02012	.000	.1058	.2382

VAR00001
Tukey HSD

Multiple Comparisons

(I) time	(J) time	Mean Difference (I-J)	Std. Error	Sig.	95% Confidence Interval	
					Lower Bound	Upper Bound
Figure 6D						
0	5	-.23467 *	.02028	.000	-.3014	-.1679
	10	-.82533 *	.02028	.000	-.8921	-.7586
	30	-.68733 *	.02028	.000	-.7541	-.6206
	60	-.46233 *	.02028	.000	-.5291	-.3956
5	0	.23467 *	.02028	.000	.1679	.3014
	10	-.59067 *	.02028	.000	-.6574	-.5239
	30	-.45267 *	.02028	.000	-.5194	-.3859
	60	-.22767 *	.02028	.000	-.2944	-.1609
10	0	.82533 *	.02028	.000	.7586	.8921
	5	.59067 *	.02028	.000	.5239	.6574
	30	.13800 *	.02028	.000	.0712	.2048
	60	.36300 *	.02028	.000	.2962	.4298
30	0	.68733 *	.02028	.000	.6206	.7541
	5	.45267 *	.02028	.000	.3859	.5194
	10	-.13800 *	.02028	.000	-.2048	-.0712
	60	.22500 *	.02028	.000	.1582	.2918
60	0	.46233 *	.02028	.000	.3956	.5291
	5	.22767 *	.02028	.000	.1609	.2944
	10	-.36300 *	.02028	.000	-.4298	-.2962
	30	-.22500 *	.02028	.000	-.2918	-.1582

VAR00001
Tukey HSD

Multiple Comparisons

(I) time	(J) time	Mean Difference (I-J)	Std. Error	Sig.	95% Confidence Interval	
					Lower Bound	Upper Bound
Figure 6E						
0	5	.02467	.02220	.797	-.0484	.0977
	10	-.33967 *	.02220	.000	-.4127	-.2666
	30	-.26100 *	.02220	.000	-.3341	-.1879
	60	-.37767 *	.02220	.000	-.4507	-.3046
5	0	-.02467	.02220	.797	-.0977	.0484
	10	-.36433 *	.02220	.000	-.4374	-.2913
	30	-.28567 *	.02220	.000	-.3587	-.2126
	60	-.40233 *	.02220	.000	-.4754	-.3293
10	0	.33967 *	.02220	.000	.2666	.4127
	5	.36433 *	.02220	.000	.2913	.4374
	30	.07867 *	.02220	.034	.0056	.1517
	60	-.03800	.02220	.469	-.1111	.0351
30	0	.26100 *	.02220	.000	.1879	.3341
	5	.28567 *	.02220	.000	.2126	.3587
	10	-.07867 *	.02220	.034	-.1517	-.0056
	60	-.11667 *	.02220	.003	-.1897	-.0436
60	0	.37767 *	.02220	.000	.3046	.4507
	5	.40233 *	.02220	.000	.3293	.4754
	10	.03800	.02220	.469	-.0351	.1111
	30	.11667 *	.02220	.003	.0436	.1897

data
Tukey HSD

Table W1. (*continued*)

Multiple Comparisons

(I) time	(J) time	Mean Difference (I-J)	Std. Error	Sig.	95% Confidence Interval	
					Lower Bound	Upper Bound
Figure 6F						
0	5	-.43533*	.01941	.000	-.4992	-.3715
	10	-.83733*	.01941	.000	-.9012	-.7735
	30	-.77067*	.01941	.000	-.8345	-.7068
	60	-.78267*	.01941	.000	-.8465	-.7188
5	0	.43533*	.01941	.000	.3715	.4992
	10	-.40200*	.01941	.000	-.4659	-.3381
	30	-.33533*	.01941	.000	-.3992	-.2715
	60	-.34733*	.01941	.000	-.4112	-.2835
10	0	.83733*	.01941	.000	.7735	.9012
	5	.40200*	.01941	.000	.3381	.4659
	30	.06667*	.01941	.040	.0028	.1305
	60	.05467	.01941	.104	-.0092	.1185
30	0	.77067*	.01941	.000	.7068	.8345
	5	.33533*	.01941	.000	.2715	.3992
	10	-.06667*	.01941	.040	-.1305	-.0028
	60	-.01200	.01941	.969	-.0759	.0519
60	0	.78267*	.01941	.000	.7188	.8465
	5	.34733*	.01941	.000	.2835	.4112
	10	-.05467	.01941	.104	-.1185	.0092
	30	.01200	.01941	.969	-.0519	.0759
data						
Tukey HSD						

Multiple Comparisons

(I) 1 = 0nm, 2 = 20nm, 3 = 0nm+Wnt3a mAb, 4 = 20nm+Wnt3a mAb, 5 = 0nm+Wnt5a mAb, 6 = 20nm+Wnt5a mAb	(J) 1 = 0nm, 2 = 20nm, 3 = 0nm+Wnt3a mAb, 4 = 20nm+Wnt3a mAb, 5 = 0nm+Wnt5a mAb, 6 = 20nm+Wnt5a mAb	Mean Difference (I-J)	Std. Error	Sig.	95% Confidence Interval	
					Lower Bound	Upper Bound
Figure 7B						
1	2	−53.00000*	4.10916	.000	−65.4984	−40.5016
	3	-.33333	4.10916	1.000	−12.8317	12.1651
	4	−49.50000*	4.10916	.000	−61.9984	−37.0016
	5	−4.50000	4.10916	.879	−16.9984	7.9984
	6	−13.33333*	4.10916	.031	−25.8317	-.8349
2	1	53.00000*	4.10916	.000	40.5016	65.4984
	3	52.66667*	4.10916	.000	40.1683	65.1651
	4	3.50000	4.10916	.955	−8.9984	15.9984
	5	48.50000*	4.10916	.000	36.0016	60.9984
	6	39.66667*	4.10916	.000	27.1683	52.1651
3	1	.33333	4.10916	1.000	−12.1651	12.8317
	2	−52.66667*	4.10916	.000	−65.1651	−40.1683
	4	−49.16667*	4.10916	.000	−61.6651	−36.6683
	5	−4.16667	4.10916	.910	−16.6651	8.3317
	6	−13.00000*	4.10916	.038	−25.4984	-.5016
4	1	49.50000*	4.10916	.000	37.0016	61.9984
	2	−3.50000	4.10916	.955	−15.9984	8.9984
	3	49.16667*	4.10916	.000	36.6683	61.6651
	5	45.00000*	4.10916	.000	32.5016	57.4984
	6	36.16667*	4.10916	.000	23.6683	48.6651
5	1	4.50000	4.10916	.879	−7.9984	16.9984
	2	−48.50000*	4.10916	.000	−60.9984	−36.0016
	3	4.16667	4.10916	.910	−8.3317	16.6651
	4	−45.00000*	4.10916	.000	−57.4984	−32.5016
	6	−8.83333	4.10916	.290	−21.3317	3.6651
6	1	13.33333*	4.10916	.031	.8349	25.8317
	2	−39.66667*	4.10916	.000	−52.1651	−27.1683
	3	13.00000*	4.10916	.038	.5016	25.4984
	4	−36.16667*	4.10916	.000	−48.6651	−23.6683
	5	8.83333	4.10916	.290	−3.6651	21.3317
VAR00001						
Tukey HSD						

Table W1. (*continued*)

Multiple Comparisons

(I) 1 = 0nm, 2 = 20nm, 3 = 0nm+NSC23766, 4 = 20nm+NSC23766, 5 = 0nm+Y-27632, 6 = 20nm+Y-27632	(J) 1 = 0nm, 2 = 20nm, 3 = 0nm+NSC23766, 4 = 20nm+NSC23766, 5 = 0nm+Y-27632, 6 = 20nm+Y-27632	Mean Difference (I-J)	Std. Error	Sig.	95% Confidence Interval	
					Lower Bound	Upper Bound
Figure 7D						
1	2	−51.00000*	2.31541	.000	−58.0425	−43.9575
	3	−4.16667	2.31541	.481	−11.2092	2.8759
	4	−15.50000*	2.31541	.000	−22.5425	−8.4575
	5	−7.16667*	2.31541	.044	−14.2092	-.1241
	6	−11.00000*	2.31541	.001	−18.0425	−3.9575
2	1	51.00000*	2.31541	.000	43.9575	58.0425
	3	46.83333*	2.31541	.000	39.7908	53.8759
	4	35.50000*	2.31541	.000	28.4575	42.5425
	5	43.83333*	2.31541	.000	36.7908	50.8759
	6	40.00000*	2.31541	.000	32.9575	47.0425
3	1	4.16667	2.31541	.481	−2.8759	11.2092
	2	−46.83333*	2.31541	.000	−53.8759	−39.7908
	4	−11.33333*	2.31541	.000	−18.3759	−4.2908
	5	−3.00000	2.31541	.785	−10.0425	4.0425
	6	−6.83333	2.31541	.061	−13.8759	.2092
4	1	15.50000*	2.31541	.000	8.4575	22.5425
	2	−35.50000*	2.31541	.000	−42.5425	−28.4575
	3	11.33333*	2.31541	.000	4.2908	18.3759
	5	8.33333*	2.31541	.013	1.2908	15.3759
	6	4.50000	2.31541	.397	−2.5425	11.5425
5	1	7.16667*	2.31541	.044	.1241	14.2092
	2	−43.83333*	2.31541	.000	−50.8759	−36.7908
	3	3.00000	2.31541	.785	−4.0425	10.0425
	4	−8.33333*	2.31541	.013	−15.3759	−1.2908
	6	−3.83333	2.31541	.570	−10.8759	3.2092
6	1	11.00000*	2.31541	.001	3.9575	18.0425
	2	−40.00000*	2.31541	.000	−47.0425	−32.9575
	3	6.83333	2.31541	.061	-.2092	13.8759
	4	−4.50000	2.31541	.397	−11.5425	2.5425
	5	3.83333	2.31541	.570	−3.2092	10.8759

VAR00001
Tukey HSD

Multiple Comparisons

(I) 1 = 0nm, 2 = 20nm, 3 = 0nm+Wnt3a mAb, 4 = 20nm+Wnt3a mAb, 5 = 0nm+Wnt5a mAb, 6 = 20nm+Wnt5a mAb	(J) 1 = 0nm, 2 = 20nm, 3 = 0nm+Wnt3a mAb, 4 = 20nm+Wnt3a mAb, 5 = 0nm+Wnt5a mAb, 6 = 20nm+Wnt5a mAb	Mean Difference (I-J)	Std. Error	Sig.	95% Confidence Interval	
					Lower Bound	Upper Bound
Figure 8B						
1	2	−71.83333*	3.48250	.000	−82.4257	−61.2410
	3	1.00000	3.48250	1.000	−9.5923	11.5923
	4	−65.33333*	3.48250	.000	−75.9257	−54.7410
	5	−1.00000	3.48250	1.000	−11.5923	9.5923
	6	−9.33333	3.48250	.109	−19.9257	1.2590
2	1	71.83333*	3.48250	.000	61.2410	82.4257
	3	72.83333*	3.48250	.000	62.2410	83.4257
	4	6.50000	3.48250	.441	−4.0923	17.0923
	5	70.83333*	3.48250	.000	60.2410	81.4257
	6	62.50000*	3.48250	.000	51.9077	73.0923
3	1	−1.00000	3.48250	1.000	−11.5923	9.5923
	2	−72.83333*	3.48250	.000	−83.4257	−62.2410
	4	−66.33333*	3.48250	.000	−76.9257	−55.7410
	5	−2.00000	3.48250	.992	−12.5923	8.5923
	6	−10.33333	3.48250	.059	−20.9257	.2590
4	1	65.33333*	3.48250	.000	54.7410	75.9257
	2	−6.50000	3.48250	.441	−17.0923	4.0923
	3	66.33333*	3.48250	.000	55.7410	76.9257
	5	64.33333*	3.48250	.000	53.7410	74.9257
	6	56.00000*	3.48250	.000	45.4077	66.5923

Table W1. (*continued*)

5	1	1.00000	3.48250	1.000	−9.5923	11.5923
	2	−70.83333*	3.48250	.000	−81.4257	−60.2410
	3	2.00000	3.48250	.992	−8.5923	12.5923
	4	−64.33333*	3.48250	.000	−74.9257	−53.7410
	6	−8.33333	3.48250	.191	−18.9257	2.2590
6	1	9.33333	3.48250	.109	−1.2590	19.9257
	2	−62.50000*	3.48250	.000	−73.0923	−51.9077
	3	10.33333	3.48250	.059	-.2590	20.9257
	4	−56.00000*	3.48250	.000	−66.5923	−45.4077
	5	8.33333	3.48250	.191	−2.2590	18.9257

VAR00001
Tukey HSD

Multiple Comparisons

(I) 1 = 0nm, 2 = 20nm, 3 = 0nm+NSC23766, 4 = 20nm+NSC23766, 5 = 0nm+Y-27632, 6 = 20nm+Y-27632	(J) 1 = 0nm, 2 = 20nm, 3 = 0nm+NSC23766, 4 = 20nm+NSC23766, 5 = 0nm+Y-27632, 6 = 20nm+Y-27632	Mean Difference (I-J)	Std. Error	Sig.	95% Confidence Interval	
					Lower Bound	Upper Bound
Figure 8D						
1	2	−78.00000*	3.68053	.000	−89.1947	−66.8053
	3	−4.16667	3.68053	.864	−15.3613	7.0280
	4	−5.50000	3.68053	.670	−16.6947	5.6947
	5	3.16667	3.68053	.953	−8.0280	14.3613
	6	−11.00000	3.68053	.056	−22.1947	.1947
2	1	78.00000*	3.68053	.000	66.8053	89.1947
	3	73.83333*	3.68053	.000	62.6387	85.0280
	4	72.50000*	3.68053	.000	61.3053	83.6947
	5	81.16667*	3.68053	.000	69.9720	92.3613
	6	67.00000*	3.68053	.000	55.8053	78.1947
3	1	4.16667	3.68053	.864	−7.0280	15.3613
	2	−73.83333*	3.68053	.000	−85.0280	−62.6387
	4	−1.33333	3.68053	.999	−12.5280	9.8613
	5	7.33333	3.68053	.370	−3.8613	18.5280
	6	−6.83333	3.68053	.447	−18.0280	4.3613
4	1	5.50000	3.68053	.670	−5.6947	16.6947
	2	−72.50000*	3.68053	.000	−83.6947	−61.3053
	3	1.33333	3.68053	.999	−9.8613	12.5280
	5	8.66667	3.68053	.205	−2.5280	19.8613
	6	−5.50000	3.68053	.670	−16.6947	5.6947
5	1	−3.16667	3.68053	.953	−14.3613	8.0280
	2	−81.16667*	3.68053	.000	−92.3613	−69.9720
	3	−7.33333	3.68053	.370	−18.5280	3.8613
	4	−8.66667	3.68053	.205	−19.8613	2.5280
	6	−14.16667*	3.68053	.007	−25.3613	−2.9720
6	1	11.00000	3.68053	.056	-.1947	22.1947
	2	−67.00000*	3.68053	.000	−78.1947	−55.8053
	3	6.83333	3.68053	.447	−4.3613	18.0280
	4	5.50000	3.68053	.670	−5.6947	16.6947
	5	14.16667*	3.68053	.007	2.9720	25.3613

VAR00001
Tukey HSD

* The mean difference is significant at the 0.05 level.